EXPERIMENTAL STUDY OF REINFORCED CONCRETE STEPPED BEAMS

By

Zahraa Abd Al-hussein Musa

B.Sc. in Civil Engineering, 2017

A thesis submitted in partial fulfillment

of the requirements for the Master of Science

degree in Civil Engineering

The University of Misan

February 2021

Thesis Supervisor: Prof. Dr. Abdulkhaliq Abdulyimah Jaafer

بسم الله الرحمن الرحيم

﴿وَلَقَدْ آتَيْنَا دَاوُودَ وَسُلَيْمَانَ عِلْمًا وَقَالَا الْحَمْدُ لِلَّهِ الَّذِي فَضَّلَنَا عَلَى كَثِيرٍ مِنْ عِبَادِهِ الْمُؤْمِنِينَ﴾

سورة النمل الآية ١٥

صدق الله العلي العظيم

DEDICATION

I dedicate this work to the spirit of my father ask God to dwell in

paradise.

To whom stood beside me and took care of me over the years, to my

mother

sisters,

brothers

and close friend

ACKNOWLEDGEMENTS

ABSTRACT

The present study aims to investigate the structural behavior of concrete stepped beams. The experimental work consisted of fourteen stepped beams with dimensions of width× height × length (b× h× l) to be 150 mm × 300 mm × 2300 mm were tested under four-point bending . In this work, three variables were studied, the first was compressive strength, which includes two values of compressive strength, 40 MPa as a normal compressive strength and 85 MPa as a high compressive strength. The second variable was the details of the steel reinforcement at the stepped joint where a diameter of 8 mm was used. Two details were used in the first model, rebar with horizontal and vertical distances of 30 and 40 mm respectively, in the second model with horizontal, vertical and slope distances of 80, 75 and 50 mm respectively, while the third variable was the external strengthening by cotton belt (one or two layers of cotton belt layer) and carbon fiber reinforced polymer sheet (CFRP), 6 models with cotton belt by different strengthening styles and 2 models with carbon fiber sheet. The behavior of stepped beam was examined by crack patterns, first crack load, final loads, load deflection response, and strains distribution.

The experimental results showed an increase in final loads up to 253.84% for internal reinforcement with high compressive strength. As for the beams strengthening with cotton belt for high strength concrete and beams strengthen with CFRP sheet for normal strength concrete, they achieved an increase in final loads of 120.5% and 62.15% compared to unstrengthen reference concrete stepped beams respectively. Moreover, these strengthening beams exhibited less deflection at corresponding loads compared to unstrengthening reinforced concrete beams. The samples achieved energy absorption, ductility index, and initial stiffness ranging from (31.75-3100) kN.mm, (1.978-8.736) and (9.61-28.28) kN /

mm, respectively. The test result also showed increases in the first crack load of up to (129.68)% in the internally reinforced beams compared to the reference beams.

TABLE OF CONTENT

LIST OF TABLES

LIST OF FIGURES

LIST OF SYMBOLS

f_t Tensile strength in MPa

f_r Modulus of rupture in MPa

ε Strain

fc' Cylinder concrete compressive strength in MPa

fcu   Cube Compressive Strength in MPa

fy   Yield strength in MPa

Δy Yield deflection in mm

py   Yield load in kN

$\mu\Delta$ Ductlity index

ABBREVIATION

ASTM   American Society for Testing and Materials

ACI   American Concrete Institute

AFRP   Aramid Fiber Reinforced Polymer

BS   British Standard

CFRP   Carbon Fiber Reinforced Polymer

FRP   Fiber Reinforced Polymer

GFRP   Glass Fiber Reinforced Polymer

HSC   High Strength Concrete

RC   Reinforced Concrete

RCHBs   Reinforced Concrete Haunched Beams

SB   Stepped Beam

SP   Superplasticizer

STM   Strut and Tie model

W/C   Water to Cement ratio

EBR   Externally Bonded Reinforced

NSM   Near Surface Mounted

R.O   Reverse Osmosis

CHAPTER ONE
INTRODUCTION

1.1 General

The non-prismatic or non-uniform reinforced concrete (RC) beam is considered a special case in structural engineering. It does not have sufficient information in structural codes, this can put structural engineers in a challenge to predict how this beam will react under specific types of loads or with different geometrical variables and strengthening existence. There are different types of non-uniform beams which are utilized in structures like stepped beam, tapered beam,…etc. The stepped beam is an example of non-prismatic beams that can be used to support a split-level floor (Mohy et al., 2013). As height of the building increases it has more chance to collapse, stepped beams if provided, can transfer load to adjacent section and the chance of deflection or collapse get reduced Shree and Kumar (Shree & Kumar, 2018).

The strengthening and rehabilitation of reinforced concrete structures are the most of challenging tasks in the civil engineering field. The upgrading and retrofitting of structures are necessary for many reasons, such as increase in vehicles loads, to overcome original design or detailing errors and the deterioration that occurs during the service life of structures (Qeshta et al., 2015). Over the last three decades, significant researches had been documented on the use of different materials for the strengthening of RC structures (Qeshta et al., 2015). In these researches, different techniques and materials were used for strengthening concrete members. Generally, steel, carbon fiber reinforced polymer (CFRP), glass fiber reinforced polymer sheets (GFRP), ferrocement and sprayed concrete were the most materials used.

1.2 Stepped Beam

A Non-prismatic beams is the beam with non-constant cross-section or beams of variable cross section are a particular class of slender bodies, an object of the practitioners interest due to the possibility of optimizing their geometry with respect to specific needs. Despite the advantages that engineers can obtain from their use, non-trivial difficulties occurring in the non-prismatic beam modeling often lead to inaccurate predictions that vanish the gain of the optimization process. As a consequence, an effective non-prismatic beam modeling still represents a branch of the structural mechanics where significant improvements are required, as an example of non-prismatic beam (Balduzzi et al., 2016). Stepped beam is an example of non-prismatic beams that can be used to support a split-level floor, in various structures including buildings, foundations and bridges as shown in Figure 1.1. This application is commonly used in theaters and in private housing for aesthetic reasons. The stepped beam provides additional need for reinforcement detailing to fulfill the stress concentration at the stepped joint to prevent premature failure (Mohy et al., 2013). An appropriate application for stepped sections could be on the floor framing of high-rise buildings where the ceiling plenums are kept shallow to limit the floor-to-floor dimension. Stepped sections provide greater clearance under beams for the ducts and other mechanical systems which are often crowded into ceiling plenums. By proper selection, greater clearance may be achieved with the added benefit of reducing the weight of beams.

The behavior of non-prismatic beams is very different from ordinary prismatic beams, and current codes do not give specific provisions for the design of such beams. Frequently, actual designs are based on rule of thumb or are empirical in nature and are not adequately

backed by research findings, as a result, the design may be too conservative in certain cases while in others, critical issues may be overlooked (Tan, 2004).

Figure 1.1 Stepped footings (stepped footing)

1.3 Webbing

Webbing is a woven fabric that is available in a variety of material compositions, widths, strengths, and fibers.

Webbing appears in a multitude of operations and industrial sectors. Some common applications and associated industries include:

1. Military soft goods including parachutes, packs, cargo, and harnesses
2. Fire safety gear for fire fighters.
3. Seatbelts and harnesses for automotive.
4. Hiking and backpacking gear for sporting good retail apparel.
5. Personal protective equipment for oil and gas workers and electrical line workers (Webbing).

1.3.1 Cotton Belt

Cotton belt is one of the most common forms of webbing used in various industries. It has a number of benefits more than some types of webbings. Since it is commonly used because of its cheap price, light weight, available in the local markets and has good strength. It has flexible webbing which has the ability to wrap tightly around the surfaces. It is used for lifting or pulling heavy weights such as concrete blocks, pipelines, etc. Figure 1.2 shows the webbing. Some of the properties of this webbing are:

(a) High Strength.

(b) Low Elasticity – Stretch and Shrink.

(c) Moderately Absorbing.

(d) Moderate Elongation.

(e) Moderate Cut and Abrasion Resistance.

(f) Low Temperature Resistance.

Figure 1.2 Webbing (Webbing).

1.4 Fiber Reinforced Polymers

Fiber-reinforced polymer (FRP) materials are an attractive new material for structural engineers in the field of concrete construction, use especially for strengthening materials for reinforced concrete (RC) beams. FRP is a composite material consisting of polymer matrix and high strength fibers. The matrix is used to bind the fibers together, transfer forces between the fibers and protect the fibers from external mechanical and environmental damage. It is important that the matrix has the ability to withstand a higher stress than the fiber, otherwise cracks will occur in the matrix before the fibers are broken and the fibers will be unprotected (Dhiyaa Hamoodi Mohammed, 2007). The mostly FRPs used in civil engineering applications are glass fiber reinforced polymer (GFRP), carbon fiber reinforced polymer (CFRP), and aramid fiber reinforced polymer (AFRP).

All the three types of FRP composites, namely, GFRP, CFRP and AFRP, have been used to strengthen the RC structures in both laboratory research activities and engineering practice. Table 1.1 presents typical properties of FRP composites. It should be noted that the ranges listed in this table are indicative, and a specific product may have characteristics outside the ranges listed here, particularly when the fiber content differs from the bands listed here. It should also be noted that when discussing the modulus of elasticity and tensile strength of FRP composite formed in a wet laying process, it is generally difficult to control or accurately define the thickness of FRP composite. This has led to the use of the fiber sheet thickness or a nominal thickness as recommended by the manufacturer (Yousif, 2012). FRP materials exhibit linear elastic stress behavior until rupture when loaded in direct tension. As a result, failure is

abrupt and potentially catastrophic. The stress and strain curves of both CFRP and steel are shown in Figure 1.3 (Mohammed, 2007).
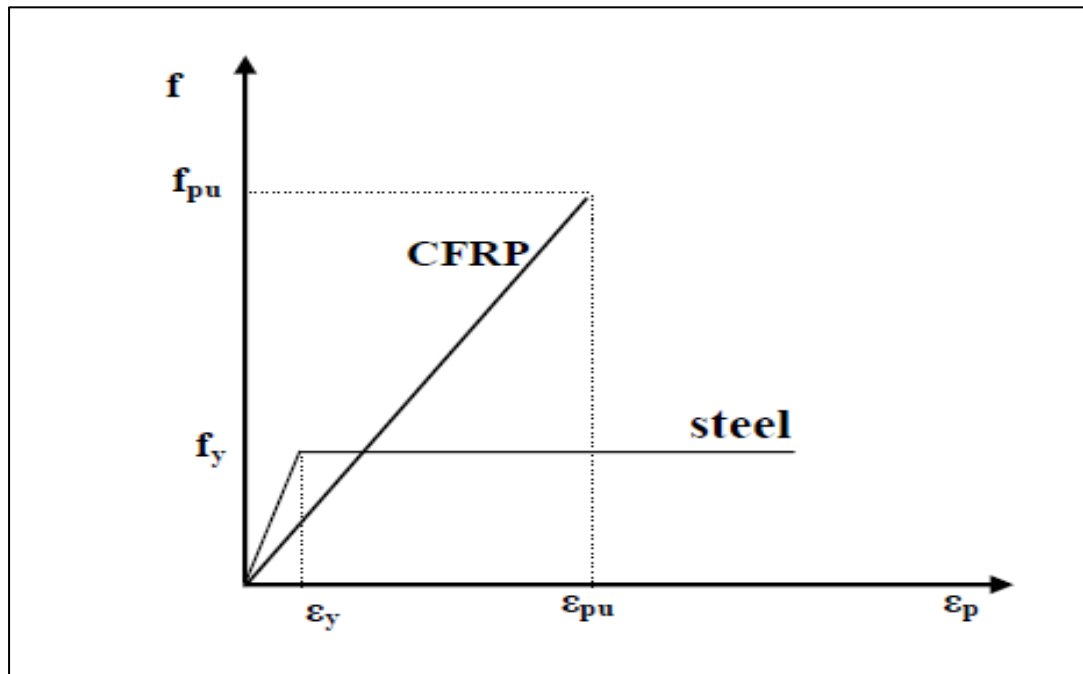
Figure 1.3 Stress-strain curves for CFRP and steel (Mohammed, 2007).

Table 1.1 Typical mechanical properties of GFRP, CFRP and AFRP composites (Yousif, 2012).

Tensile strength (MPa)	Longitudinal tensile modulus (GPa) of fiber	Density (kg/m^3)	Fiber content (% by weight)	Unidirectional advanced composite materials
400-1800	20-55	1600-2000	50-80	Glass fiber/polyester GFRP laminates
1200-2250	120-250	1600-1900	65-75	Carbon/epoxy CFRP laminate
1000-1800	40-125	1050-1250	60-70	Aramid/epoxy AFRP laminate

1.5 High Strength Concrete

The definition of high-strength concrete (HSC) has changed over the years, and it is not static. The precise strength defining high-strength concrete also tends to vary by geographic location. In a 1984 American Concrete Institute (ACI) committee report (Ghosh, 2004), revised and reissued in 1992 as 6000 psi (41 MPa) was selected as a lower limit for high-strength concrete. It is not intended to imply that there is a drastic change in material properties or in production techniques that occur at this compressive strength. In reality, all changes that take place above 6000 psi (41 MPa) represent a process which starts with the lower-strength concretes and continues with high-strength concrete. ACI 363R-92 updates their state of the art report on high-strength concrete concept. In the draft update of ACI 363R-92, it defined a high-strength concrete as concrete having a specified compressive strength for design purposes more than 8000 psi (55 MPa) (Ghosh, 2004). Materials which participate in high–strength concrete proportioning are, supplementary cementitious materials, fly ash, silica fume and some other mineral admixtures, aggregates of the best quality and of high compressive strengths which include dolomites, granites, quartz etc., as well as superplasticizers or some other types of chemical admixtures. Water to cement ratio in high strength concretes is lower and it varies from 0.22 to 0.40 (Kovacevic & Dzidic, 2018). Figure 1.4 showed that the North Boulevard Bridge in Louisiana was made from high strength concrete (de Rooij & Mendonça Filho, 2015).

High strength concrete (HSC) has been successfully used in many countries across the world in high-rise buildings. High strengths are also used in bridge applications, as well as dams, grand stand roofs, marine

foundations, heavy duty industrial floors and parking garages etc. (Gokul & Indira, 2020).

High–strength concrete (HSC) was developed as better and as structural material of higher quality when compared to normal strength concrete. Therefore it has many benefits in both performance and cost efficiency. So HSC advantages are reduction in structural element size, reduction in amount of longitudinal reinforcement and compression members, focusing on slenderer columns, higher strength and better performance leads to larger spans and decrease of total number of beams, columns etc., decreased time necessary for concrete's formwork due to early strength development, decrease in concrete cover due to lower permeability, lower creep and shrinkage with higher resistance for freezing and thawing, increased resistance to very aggressive environments, decreased permanent action of self–weight of structure, decreased maintenance, and repair costs and greater stiffness due to higher modulus of elasticity with high compressive and flexural strengths (Kovacevic & Dzidic, 2018).

Figure 1.4 The North Boulevard Bridge in Louisiana was made from high strength concrete (de Rooij & Mendonça Filho, 2015).

1.6 Research Objectives

The objective of this study is to examine the behavior of stepped beam. The main purposes of this work are:

1- To investigate the effect of concrete compressive strength on the characteristics of the stepped beam by using two types of concrete (normal and high strength).

2- To study the effect of internal reinforcement details at the middle third region of stepped beam by using closed stirrups and longitudinal steel bars.

3- To study the effect of strengthening of RC stepped beam by using cotton webbing (cotton belt strips) and CFRP sheets on the behavior of specimens.

1.7 Thesis Layouts

The study is presented in five chapters, they are as follows:

1. Chapter one is introduction about the concepts of stepped beam, webbing, fiber reinforced polymer, high strength concrete and the objectives of research.

2. Chapter two presents literature review concerning the previous studied have dealt with strengthened of stepped beam, dapped end beam and haunch beams.

3. Chapter three revolves around all the materials have been used for casting, and strengthening specimens. Characteristics of these materials are also explained in this chapter. The experimental program, description of the tested specimens, the test program and setup, and concrete mix design were described too.

4. Chapter four presents analysis and discusses the obtained results from the experimental work.

5. Chapter five provides summary for the research, conclusions with recommendations for future works.

CHAPTER TWO

LITERATURE REVIEW

2.1 Introduction

This chapter presents an overview of the experimental and analytical studies that have dealt with reinforced concrete stepped beams. These research studies are primarily aimed at studying the behavior of stepped reinforced concrete beams. They mostly focused on the behavior of reinforced concrete dapped end beams and haunched beams.

2.2 Strengthening of Stepped Beam

Afefy et al. (Afefy et al., 2013) conducted an experimental study for-rehabilitation of defected reinforced concrete (RC) stepped beams by using CFRP. Seven RC beams were fabricated, molded then tested until failure. These specimens were divided into two groups; the first group involved three beams represent the non-strengthened specimens. The second group included four beams which were strengthened by CFRP sheets. The mode of failure, ultimate capacity, cracking load, load-deflection relationship, toughness, and initial stiffness, ultimate developed strains in the main reinforcing bars at both portions of the beam, strain of concrete at compressive face and ultimate developed tensile strains in the CFRP strips were the main characteristics reported at this study. The results showed defects in the reinforcement details of the stepped beam could cause a premature failure with an eventual significant drop in ultimate capacity up to 77% compared with that of the correctly detailed beam. From the viewpoint of all failure modes, using haunch was preferable than sharp changing of the concrete section. Cross-sectional

analysis showed good agreement with experiment results related to the restoration of the yielding capacity of defected internal reinforcement of the stepped beams. The adopted CFRP strengthening system could restore the ultimate capacity of the defected beam which was placed according to strut and tie model. The behavior of strengthened beams by was 15 % more than the properly detailed stepped beam. It was not guaranteed that the technique of strengthening CFRP always increases the ultimate capacity of defected beam. The configuration of CFRP which depended on the rigorous analysis, represented the critical limit for obtained good results. Figure 2.1 Concrete dimensions and reinforcement detailing of the stepped beam.
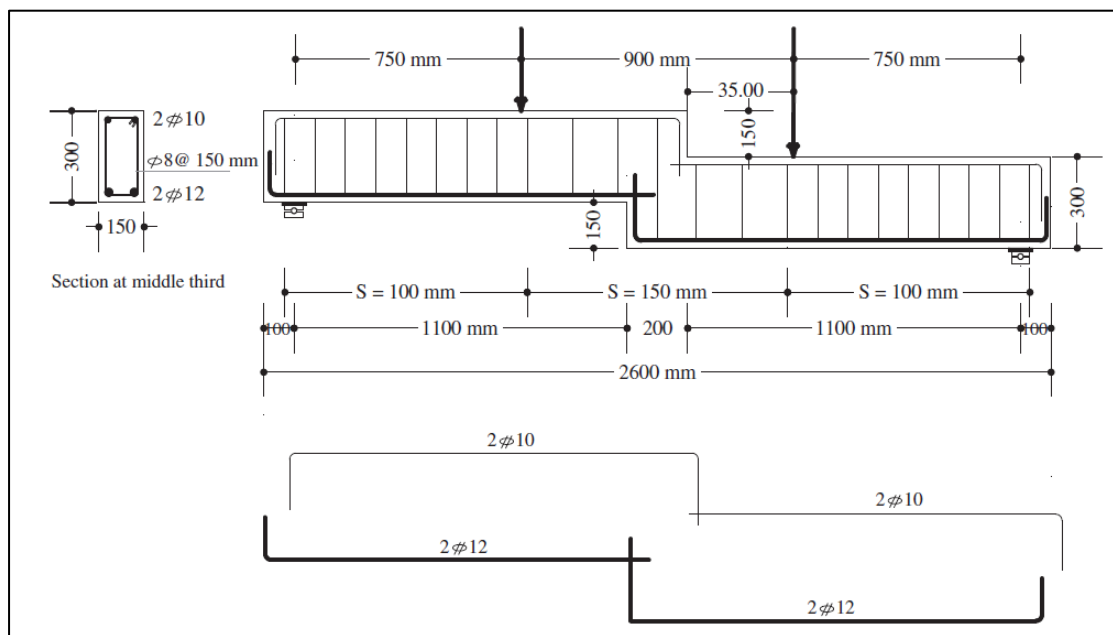
Figure 2.1 Concrete dimensions and reinforcement detailing of the stepped beam (Afefy et al., 2013)

Hussain and Safiq (Hussain & Safiq, 2016) performed an experimental work to study the performance of stepped reinforcement concrete beams. The aim of this study was to present and analyze of stepped beams strengthened with carbon fiber reinforced polymer subjected to flexural loading. Eight beams were used to achieve that purpose which divided into two groups. Group A contained two

unstrengthened beams represented as control beams that had two different arrangements of steel reinforcement in the bottom corner; one at an angle $45°$ and the other at an angle $90°$. The second group B contained six beams representing the stepped beam strengthened with CFRP sheets; three of them with angle $45°$ and the other three with angle $90°$. The results showed that using carbon fiber reinforced polymer CFRP will provides additional strengthening flexural reinforcement, the reliability for this material application depends on how good they are bonded to concrete beam to transfer the stress from concrete to CFRP laminate. Figure 2.2 Stepped concrete reinforcement beam with 90◦ at the bottom
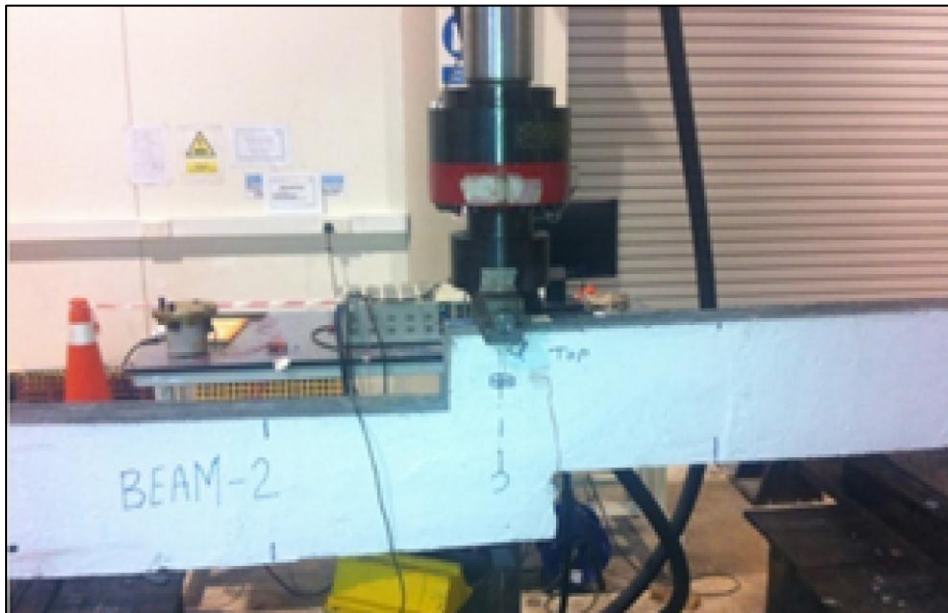
Figure 2.2 Stepped concrete reinforcement beam with 90◦ at the bottom
(Hussain & Safiq, 2016)

Shallan et al. (Shallan et al., 2017) presented an experimental and numerical investigation to study the behavior of stepped reinforced concrete beam under the effect of static load. The reinforcement and dimensions of tested beams are illustrated in Figure 2.3. An experimental the study was conducted to perform the purpose of study. Nonlinear finite element modeling conducted by utilizing ANSYS software for simulating

stepped reinforced concrete beam. A single model identical to the experimentally tested beam by using this program was prepared. Numerical study was performed to predict the maximum load carrying capacity. The behavior of the nonlinear materials, as it is related to the steel and concrete simulated appropriate constituent models. The analytical results show good agreement with the experimental results.. The tested beams were concerned in the stepped portion. The ratio of the difference between the experimental and analytical beam was 12.6% and 13.3 % for the ultimate load and deflection, respectively.
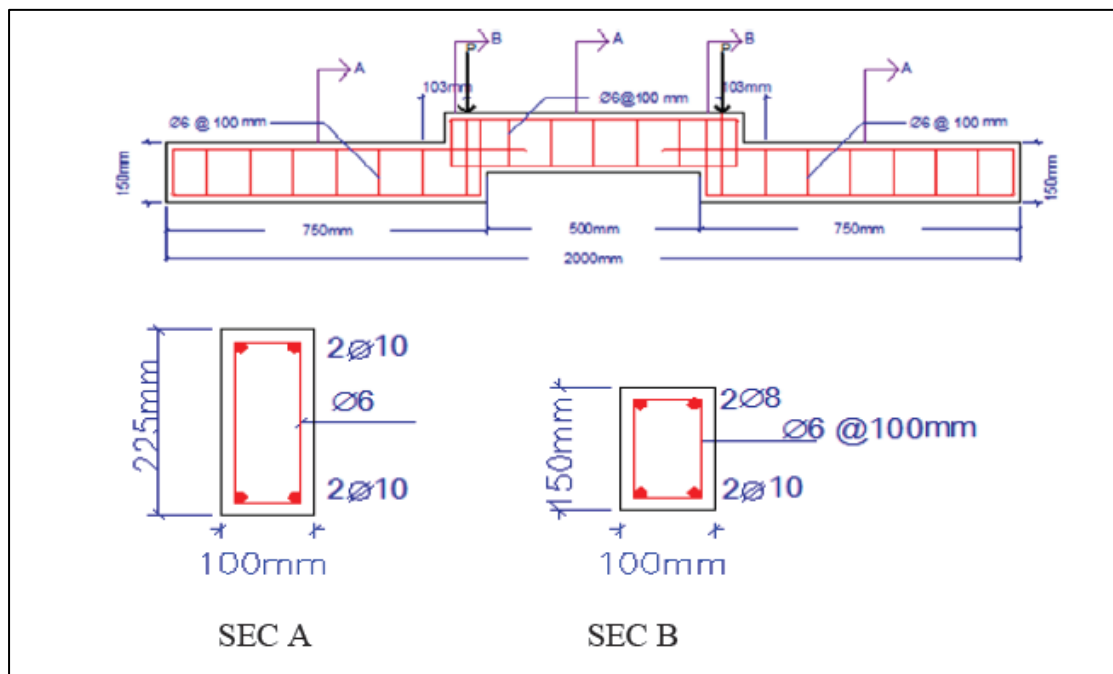
Figure 2.3 Experimental tested beam dimensions and reinforced details (Shallan et al., 2017).

Shree and Kumar (Shree & Kumar, 2018) conducted an analysis study of a stepped beam with multiple transverse cracks. Hybrid fiber reinforced concrete stepped beam was used for analytical in this study. Also, CFRP strips are used to retrofit the defected beams. CPRP strips are used in this project for retrofitting the defected beams. Stepped beams mainly avoids catastrophic failures. Vibration analysis for natural frequency and transverse crack detection are made with multiple cracks

using fracture mechanism. Also deflection tests are processed in ANSYS modeling of entire building with stepped beams, results in safe and economical benefits. Finally flexural performance of stepped beam and CFRP strengthening beam configuration along with seismic analysis is proposed.

Fayed et al. (Fayed et al., 2020) conducted an experimental and numerical study behavior of RC stepped beams with different configurations. In this research, the experimental program consists of one straight beam and seven stepped beams (SBs). Furthermore, a numerical validation is to be applied by using finite element analysis. Effects on SB behavior of additional vertical and horizontal stirrups, diagonal bars, formation of tensile rods and angle of inclination of the stepped joint were studied. Compared to the straight beam, the ultimate load reduction ratio of the SB ranged from -64.23 % to 0 %. On the one hand, as the joint drop increases, the ultimate load of the SB decreases. On the other hand, when the joint width increases, the ultimate load of the SB increases. Many of the techniques proposed for strengthening and dimensions of the stepped part have increased flexural capacity. Proposed equations of the flexural capacity of the SB were induced after examination, having taken into consideration the required parameters of the stepped beams, such as the compressive strength of the concrete, the tension and the compression steel, the dimension of the beam section, the horizontal stirrups, the diagonal bars, or the width and the drop of the stepped joint. Figure 2.4 Details of the stepped beams, dimension in cm.
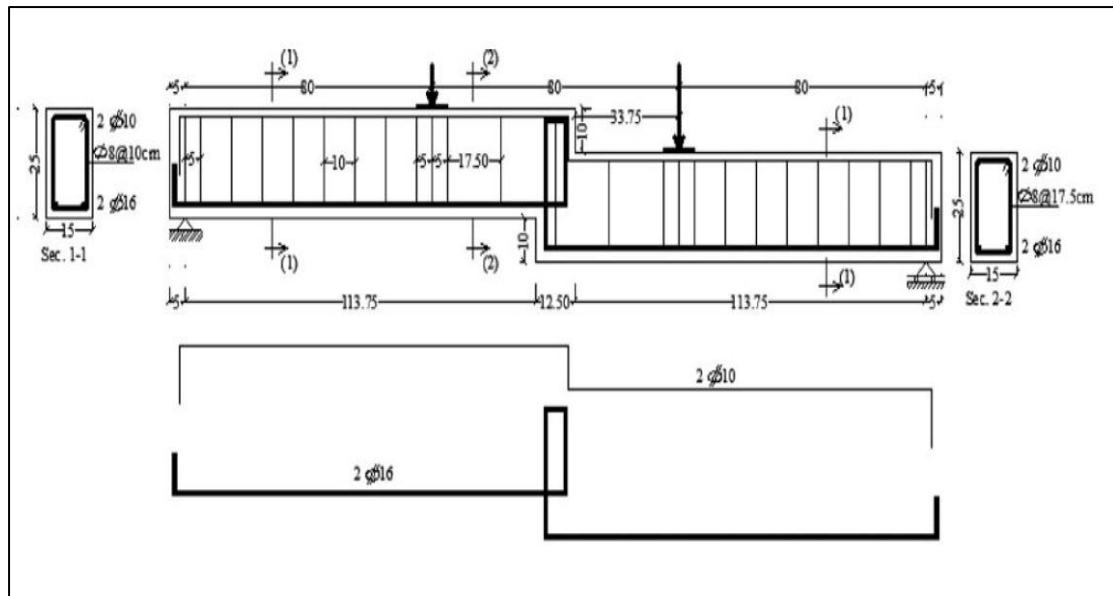
Figure 2.4 Details of the stepped beams, dimension in cm (Fayed et al., 2020)

Tan (Tan, 2004) studied the design of non-prismatic RC beams by using strut-and-tie models. Dimensions of tested specimen were shown in Figure 2.5. This study dealt with the application of strut and tied models in the analysis and design of non-prismatic reinforced concrete beams. Seven beams were designed, fabricated and tested up to failure. Test results showed that the ultimate load capacity exceeded the designed loads for all beams. The performance of non-prismatic beams with a recess across the web was satisfactory, compared to beams with equivalent transverse rectangular openings. For non-prismatic beams with a lower recess, an increase in a recess width led to decrease in stiffness and increase in beam deflection. Compared to beams with a recess in the tensile zone, non-prismatic beams with a recess in the compression zone performed better with respect to cracking patterns. Also, the strength of beams strengthened with carbon fiber reinforced polymer sheets had significantly increased. The deflection and crack widths increased rapidly thereafter leading to a sudden and non-ductile failure of the beam.
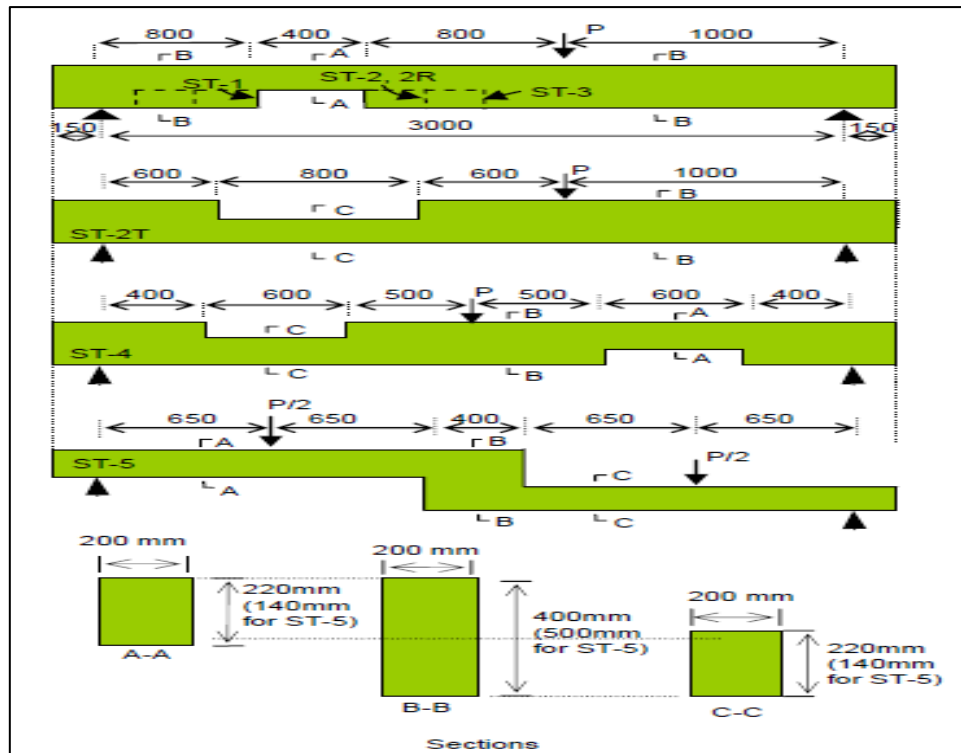
Figure 2.5 Dimensions of test beams (all dimensions in mm) (Tan, 2004).

2.3 Strengthened of Dapped End Beam

Atta and El-Shafiey (Atta & El-Shafiey, 2014) carried out an experimental study for strengthening RC dapped end beams under torsional moment. Besides the control specimen, three reinforced beams were constructed and strengthened with various techniques. These involved application of fiber reinforced polymer FRP sheets, FRP strips and external prestressed steel. The research results showed that the external prestress technique produces higher ductility than other techniques, on the other hand, the use of external prestressing and carbon fiber reinforced polymer (CFRP) wrapping to strengthen RC dapped beams subjected to torsional moment increased cracking and failure loads compared with the use of externally bonded CFRP laminate. Three dimension truss models were presented to predict the final loads of the

tested beams. The model showed a good agreement with the experimental results. Figure 2.6 showed the beam dimensions.

Figure 2.6 (a) Control beam dimensions and load position;(b) arrangement of reinforcement for tested beams (dimensions in mm) (Atta & El-Shafiey, 2014)

Sas et al. (Sas et al., 2014) presented a numerical study to obtain optimal distribution of externally bonded EBR CFRP and near surface mounted reinforcement NSM on the behavior of dapped-end beams. Dimensions and layout of the steel reinforcement were shown in Figure 2.7. To identify the most efficient configuration of CFRP used for strengthening reinforced concrete dapped-end beams, finite element models were adopted for achievement this purpose. Twenty four externally bonded EBR and NSMR configurations were prepared. The mechanical properties of the CFRP, the strengthening procedure and the inclination of the fibers with respect to the longitudinal axis were the

parameters investigated. Two cases of failure were considered. It was FRP rupture and deboning. The results indicated that higher-strength NSM FRPs could significantly increase the dapped-end beam capacity and could significantly reduce the yielding strains in reinforcement by using high-modulus fibers.
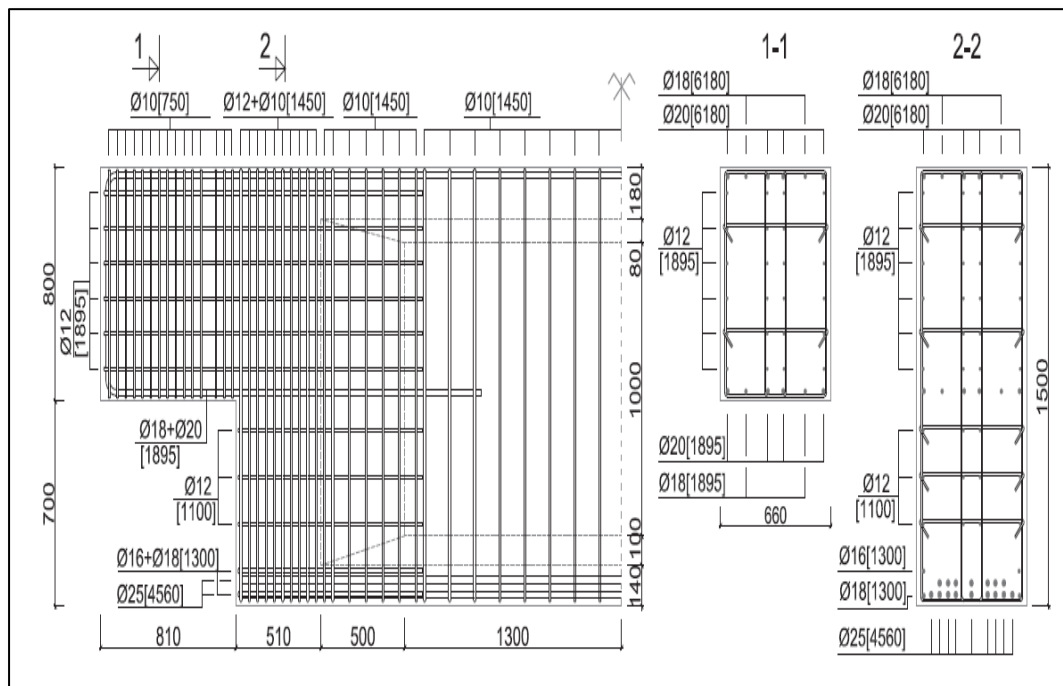
Figure 2.7 Dimensions and layout of the steel reinforcement (Sas et al., 2014).

Atta and Taman (Atta & Taman, 2016) used an external pre stressing technique and innovative method for strengthening dapped-end beams. The study presented an experimental program for eight reinforced concrete beams with dapped ends. Seven samples were strengthened by using different variations of the external prestressing technique directions: horizontal, vertical and inclined. A non-strengthened sample was investigated as a reference beam. The test results showed that the vertical external stress techniques were a very effective strengthening method to increase the capacity of beams with dapped end up to 82% compared to the control sample. A new failure pattern appeared according

to the reinforcement technique by using external horizontal prestressing and led to compression failure. In addition, a comparative study was performed to evaluate the efficacy of different reinforcement techniques. A strut-and-tie model (STM) was used in the analysis of this discontinuity in region D. A comparison of the used techniques and other past work has been made to provide a reasonable estimate of the efficacy of the results. Figure 2.8 Test setup, details of tested specimens and position of instrumentations.
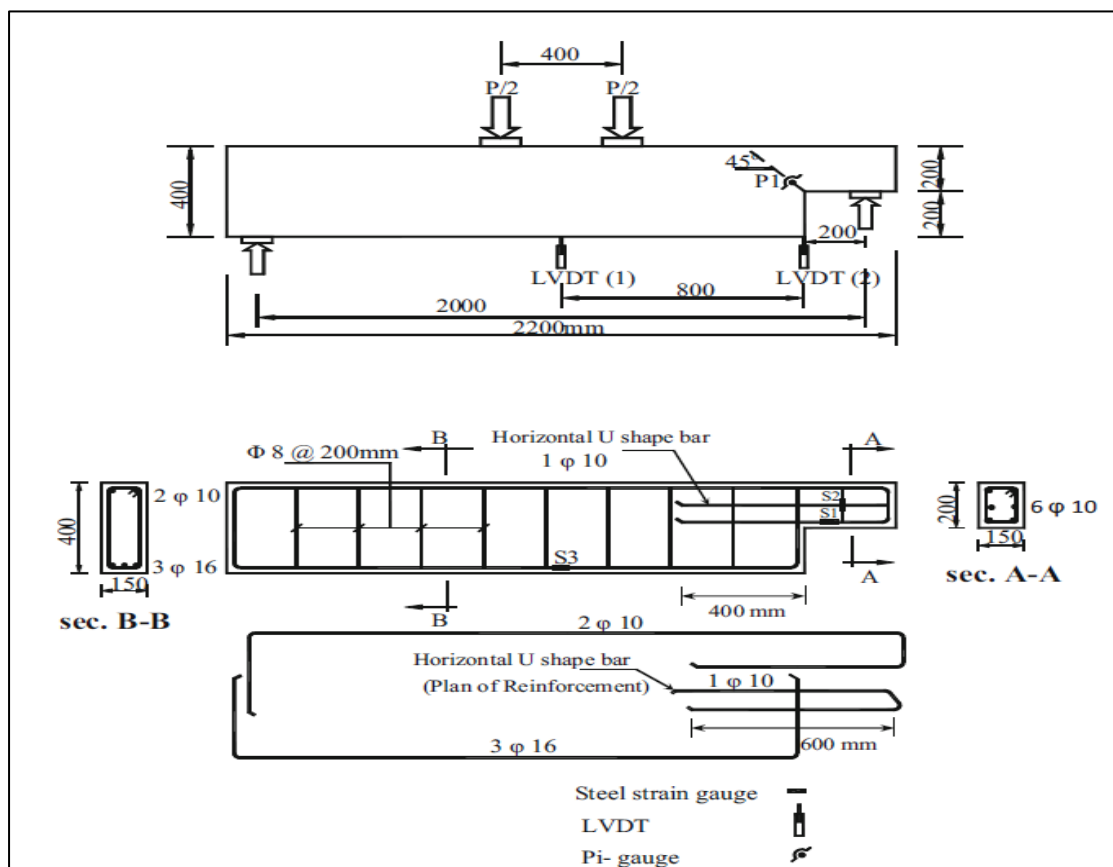
Figure 2.8 Test setup, details of tested specimens and position of instrumentations (Atta & Taman, 2016)

The efficiency of applying various external strengthening techniques to the dapped end beams was numerically evaluated by Abdel-Moniem et al. (Abdel-Moniem et al., 2018). Two-dimensional finite element model was constructed to predict the structural behavior of dapped ends strengthened by various techniques. The techniques included

external bonding of the steel angle at the re-entrant corner, un-bounded bolt anchoring, external steel plate jacketing, exterior carbon fiber wrapping and/or stripping and external inclined steel plates. The FE analysis results are then presented in terms of the ultimate load capacities, load-deflection and crack pattern at failure. Also, numerical model was found to provide better prediction of ultimate load for dapped end beams compared to strut and tie models. The steel plate jacketing method is a suitable technique for improving the behavior of dapped end. Because it has the best load capacity, besides it has a great effect on the limiting of the shear cracks in the recess corner compared with external angle and inclined bolt methods. While the bolt anchoring technique presented the better ductile behavior. Externally FRP strengthening technique was found to be a suitable method to strength of dapped end beams especially the use of horizontal CFW in both the reduced and full depth zones with inclined CFRP stripping. Because it could develop a high ductility and strength after the concrete cracked. Figure 2.9 Dimensions and reinforcement details of modeled beam.

Figure 2.9 Dimensions and reinforcement details of modeled beam
(Abdel-Moniem et al., 2018)

Experimental and numerical investigation of self-compacting reinforced concrete dapped end beams were conducted by Shakir et al. (Shakir et al., 2018). The aim of this study was to verify the behavior of self-compacted beams strengthened with CFRP sheets. The experimental program consisted of testing 14 specimens with identical dimensions (200×400×1500) mm with two values of shear span to depth ratio (a / d), namely (1.5 and 1.0). Two of these beams were considered as control beams (which provided proper details). The reinforcement of the other four beams were reduced in hanger and nib region. Other beams were intended by using different configurations of CFRP sheet as shown in Figure 2.10 Load-deflection curves and cracked specimens were used to compare the results. Reducing the (a / d) ratio from (1.5) to (1.0) for the control specimens resulted an increasing in the load capacity about of 17% and shifting the failure mode from the diagonal tension at the extended end to the diagonal tension at the reentrant corner. Reducing 50% of hanger reinforcements led to little decrease in failure load, which was about of 13 %, whereas reducing 60% of nib reinforcement caused lowering in the failure load about of 35% and 15% for (a/d) ratios of 1.5 and 1.0 ,respectively. Strengthening with CFRP sheets improved both the shear strength and the general performance of the dapped ends. The improvement in beam load capacity for strengthened hanger regions with inclined CFRP strips was in average 20%, while the vertical strip of CFRP enhanced the ultimate capacity of dapped beam with a lower percentage. They were 11% and 18% for (a/d) ratios 1.5 and 1.0, respectively .
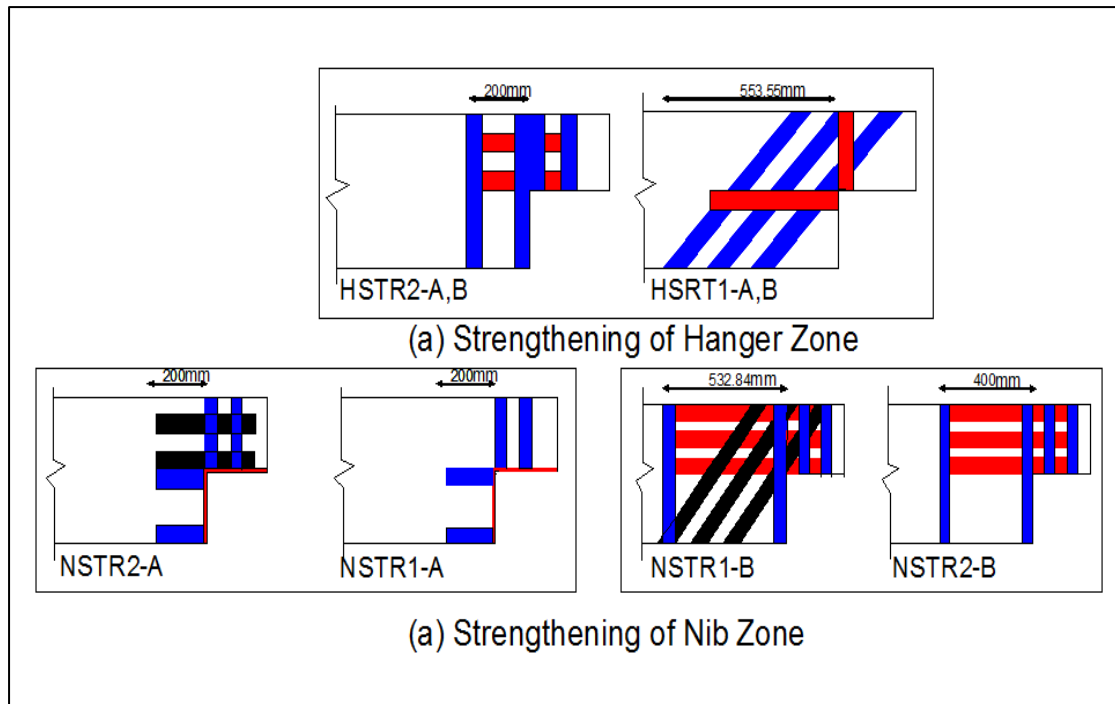
Figure 2.10 Strengthening configurations of dapped end beam
(Shakir et al., 2018).

Two strut and tie models (STM) for dapped end beams were experimentally evaluated by Soto et al. (Rentería-soto et al., 2019) two STM which were designed, the dimensions of the beam were 500 mm height by 250 mm in depth, at one end 250 mm of the total height was cut, giving a cut-off section of 250 mm per side, as shown in Figure 2.11. The proposed section was modeled in a commercial finite element software to identify the direction of the trajectory of the principal stresses. Once the values of the main stresses were obtained, the two MPT were designed, model1 (M1) has an orthogonal configuration Figure 2.12, and the second one (M2) has a strut that crosses the section change border with an inclination equal to the direction of the main stresses in the reentrant corner Figure 2.13 the results revealed the MPT diagonal exhibited better behavior than the MPT orthogonal. The displacement was smaller in M2, until the concrete exceeds its shear strength due to stirrups work in the entire section. The M2 transfers the load efficiently

because the main tensor receives the load directly, and the capacity of the steel is used because it takes the direction of the stresses. A diagonal MPT is an appropriate option, but it is necessary to study different load configurations.
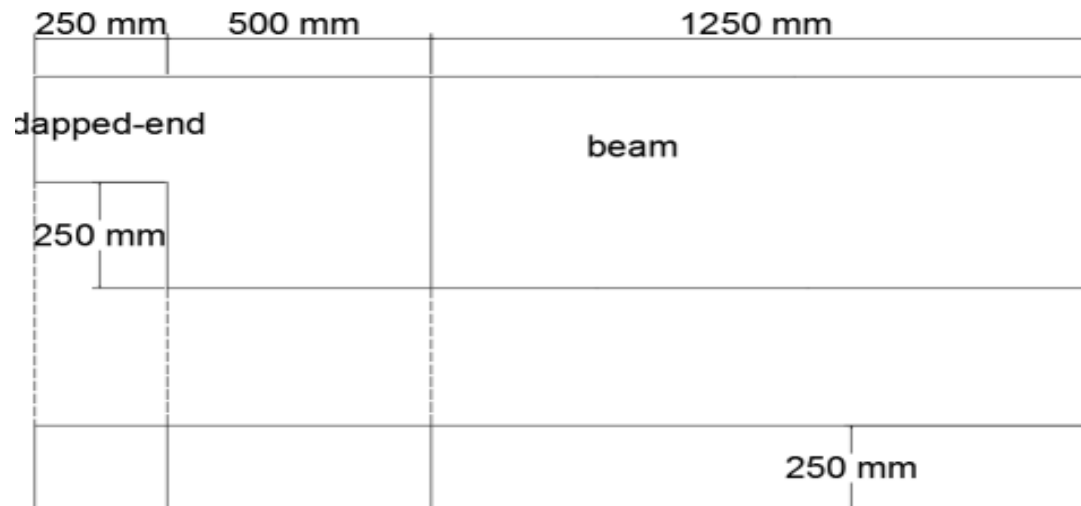
Figure 2.11 Dimensions of the specimens (Rentería-soto et al., 2019).
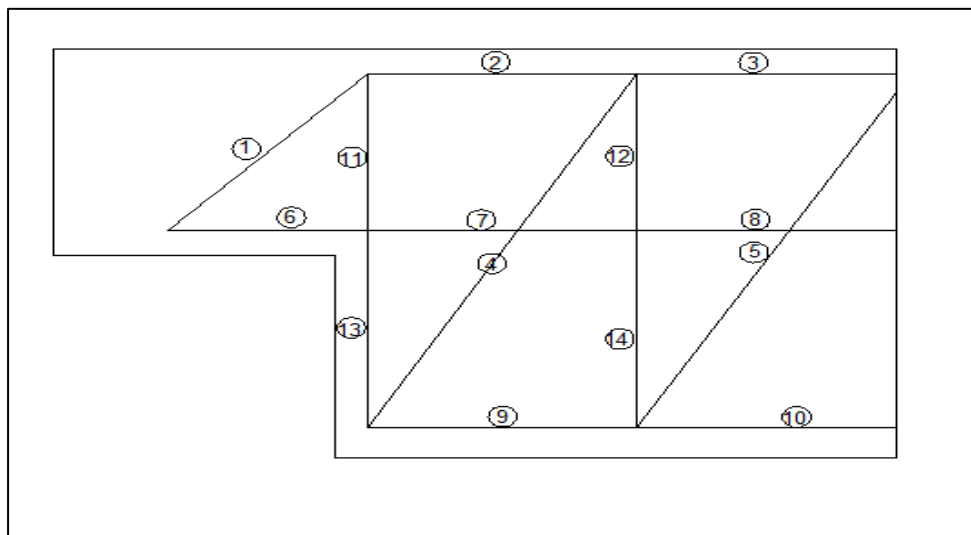
Figure 2.12 Orthogonal model M1(Rentería-soto et al., 2019).
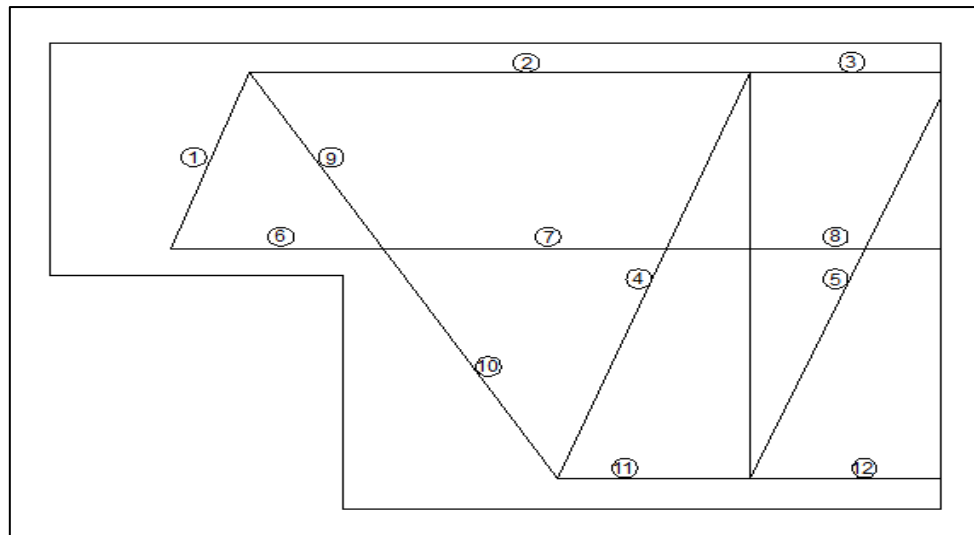
Figure 2.13 Diagonal model M2(Rentería-soto et al., 2019).

2.4 Strengthened of Haunch Beam

Jolly and Vijayan (Jolly & Vijayan, 2016) studied structural behavior of reinforced concrete haunched beam. Prismatic beams were commonly used in medium span beams. As the span increased, those beams became uneconomic due to an increase in depth. In this case, non-prismatic beams (haunched beams) were a good option for solving the problem. In this research, the structural behavior of reinforced concrete haunched beams was studied by using ANSYS and ETABS. Comparison between prismatic and haunched beams in terms of displacement and stress intensity was conducted through nonlinear static analysis. The seismic analysis was based on the time period for determining, the base shear and the inter story drift of RC frames with linear and stepped haunch beams. Deflection developed in Reinforced Concrete Haunched Beams (RCHBs) was more than compared with Prismatic beams. This increase was mainly related to the RCHBs' capacity to redistribute cracking along the length of haunched beam. The increasing capacity for deformation in non-prismatic beams was due to the arching action along the haunched length. In RCHBs, the stress intensity was 3% smaller than

that of prismatic. The presence of a non-prismatic member can affect the frame structure's seismic behavior, i.e. it decreases the structure's stiffness, which in turn reduces the base shear. Non-prismatic member presence increases significantly the lateral stiffness of buildings. Figure 2.14 Geometry, loads and boundary conditions of RCHBs.
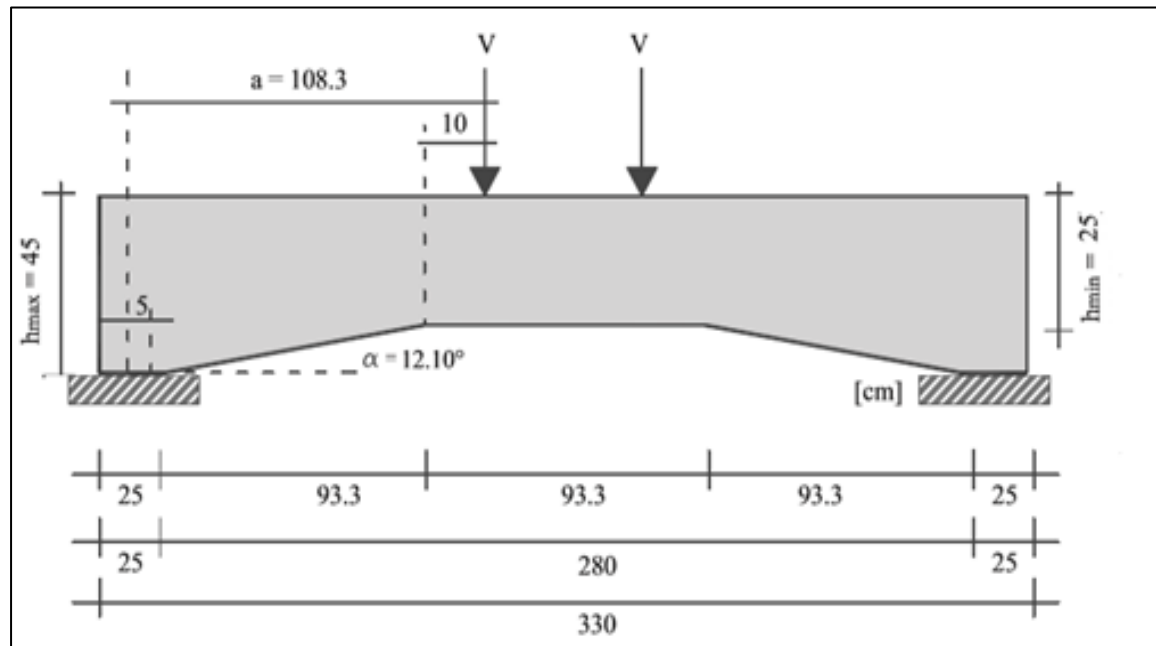
Figure 2.14 Geometry, loads and boundary conditions of RCHBs (Jolly & Vijayan, 2016)

Jaafer and Abdulghani (Jaafer & Abdulghani, 2018) presented nonlinear finite element analysis for reinforced concrete haunched beams with opening. In this research, an analysis of fourteen simply supported reinforced concrete haunched beams (RCHBs) was carried out. Members were designed to ensure the shear failure . In order to ascertain the accuracy and validity of the finite element (FE) procedure, the verification process was carried out on three solid RC haunched beams analyzed by using ANSYS software. The verification results showed a good match between FE and the experimental tests in terms of load deflection curves, load capacities, and crack patterns parametric study

was also performed through many parameters including an existence of transverse opening in the haunch zone, presence of longitudinal opening and varying the compressive strength. The result showed and confirmed that the existence of the opening led to decrease of the shear strength of these beams. Maximum reduction occurred in the longitudinal opening 125×125 mm by 39%, while the lateral opening of dimensions 100×100 mm caused 30% reduction of ultimate capacity. The presence of the opening near the vertex represented the critical location. In addition, reinforcing the opening and increasing f'c restored the loss in strength and enhanced the ductility of haunced beams. Figure 2.15 The dimension of the analyzed beam.
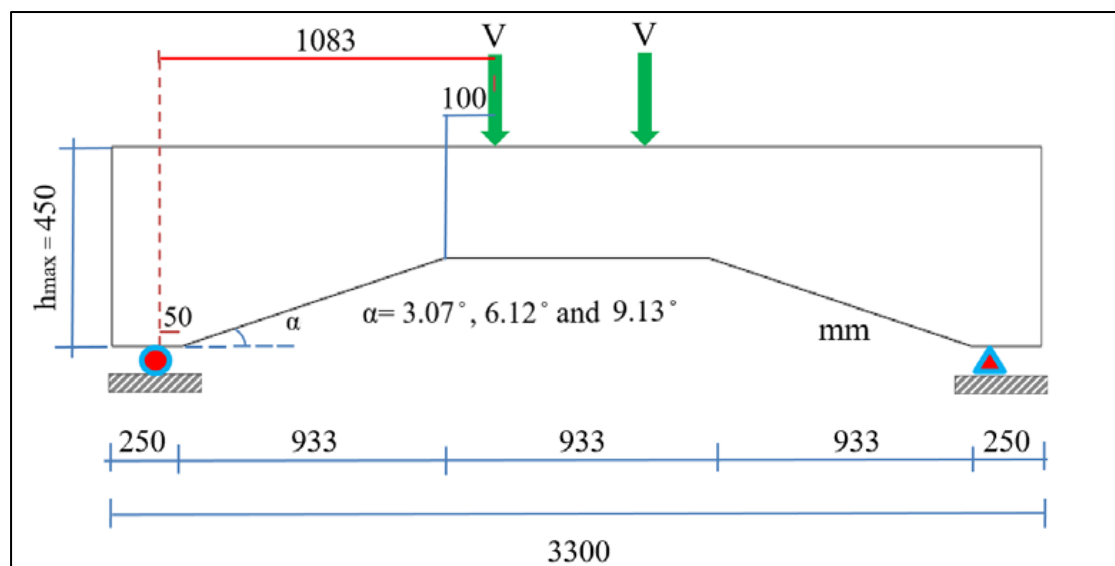
Figure 2.15 The dimension of the analyzed beam (Jaafer & Abdulghani, 2018).

Al Jawahery et al. (Al Jawahery et al., 2019) conducted an experimental investigation of rehabilitated RC haunched beams via CFRP with 3D-FE modeling analysis. The study consisted of two parts. The first part was experimental conducted on ten RCHBs and two control (prismatic) beams that designed to fail in shear. The second part concerned with finite element modeling of rehabilitated RCHBs. To form

a limit zone that exhibits all possible load capacities of rehabilitated RCHBs, a finite element based approach was proposed. FE modeling of undamaged and strengthened haunched beams by CFRP represented the maximum limit, while FE modeling of damaged beams rehabilitated by CFRP only without crack repair by epoxy represented the minimum limit. There was a good correlation between experimental and nonlinear FE results for undamaged RCHBs regarding load and deflection with correlation coefficients (R^2) of 0.8349 and 0.7923, respectively. Ultimate load capacity of all rehabilitated RCHBs by CFRP observed to be between the minimum and the maximum limits of the analyses of the FE. In addition, the load capacity of the rehabilitated beams exhibits a good correlation with the maximum limit load capacity results ($R^2 = 0.859$). This result emphasizes the importance and necessity of repair cracks before to rehabilitation with CFRP strips.

Numerical analysis of non-prismatic reinforced concrete beams strengthened by carbon fiber reinforced polymers was conducted by Ibrahim and Rad (Ibrahim & Rad, 2020). Fourteen reinforced self-compacting concrete non-prismatic (haunched) beams with or without strengthening were established. The overall length of beams was 2000 mm, depth at supports (hs) of 250 mm, width of 150 mm and different haunched angle (α) values that formed different mid-span depth (hm).

Figure 2.16 shows beams geometry, loading and supporting conditions. All beams were tested under monotonic loading up to failure. Concrete damage plasticity constitutive model used to investigate the shear strength of the non-prismatic RC beam. In addition, in order to improve the shear strength of existing RC beams, carbon fiber reinforced polymer strips were attached to the surface of concrete at critical sections. For this aim, the initial numerical model was calibrated according to data

collected from laboratory tests. A series of numerical simulations with different variables was then carried out to investigate the shear behavior. These variables were haunch angle α value and the existence of CFRP strips. Numerical results showed that changing beam geometry (haunch angle α value) had an effect on shear strength. Using CFRP strips had an obvious influence on the failure behavior of the non-prismatic RC beam structure. Finite element simulations were conducted using ABAQUS program.
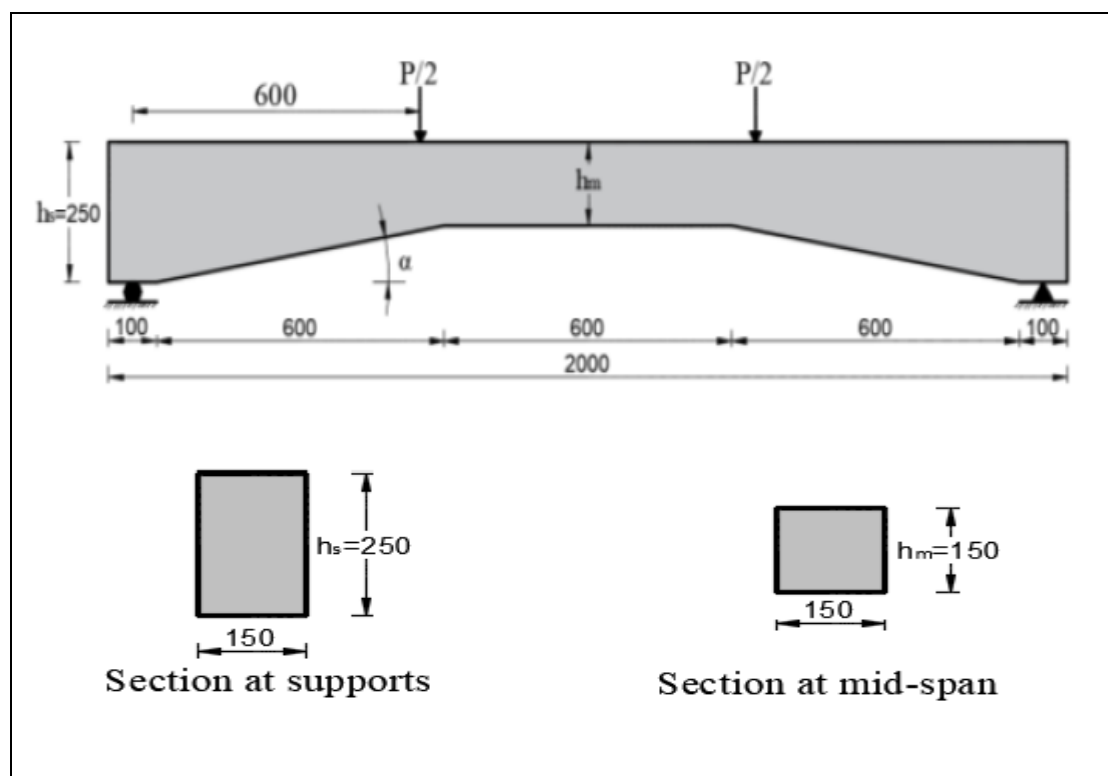
Figure 2.16 Beams geometry and loading condition(Ibrahim & Rad, 2020).

Colunga et al. (Tena-Colunga et al., 2020) carried out a strengthening of prismatic and haunched reinforced concrete beams by using light jacketing. Eight reinforced concrete beams (two prismatic and six haunched) designed and tested to fail in shear with substantial damage were presented and tested. The strengthening technique used was external

beam jacketing, consisting of a light-gauge steel wired mesh covered with a 2 cm thick grout. Beams were tested under monotonic loading. The obtained load-displacement curves for the repaired jacketed beams were compared with those obtained for the original beams. It was found that the external jacketing technique was effective, as higher deformation and load capacities were achieved for the repairing beams in comparison to the original beams. Figure 2.17 Schematic representation of geometry and testing setup for subject beams (Tena-Colunga et al., 2020).
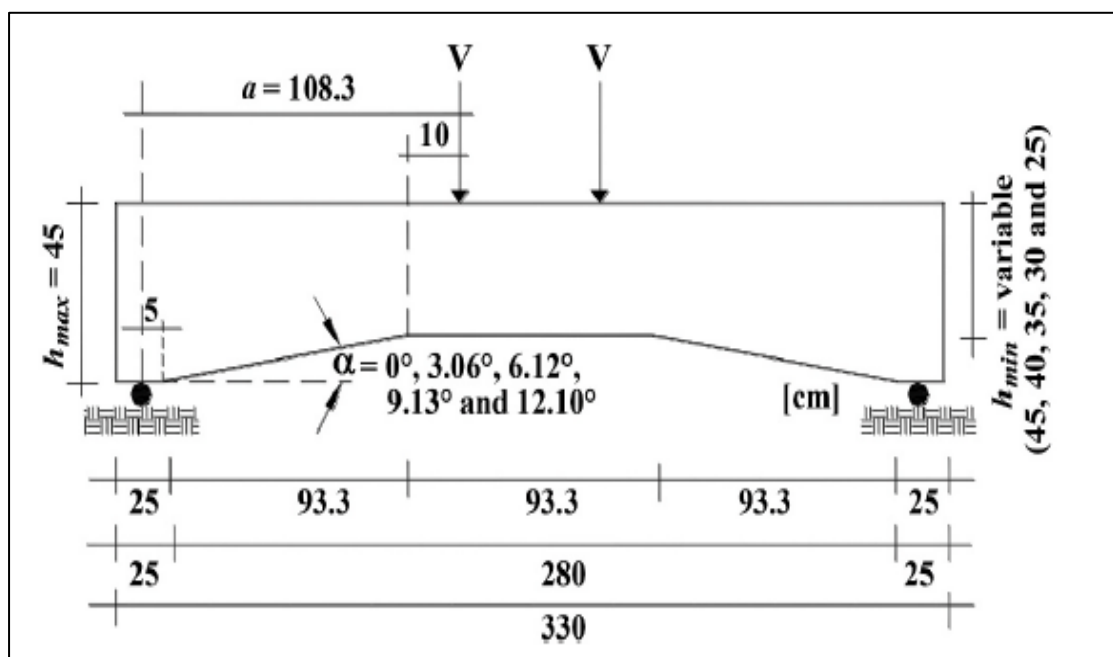
Figure 2.17 Schematic representation of geometry and testing setup for subject beams (Tena-Colunga et al., 2020).

2.5 Summary

The most previous experimental and numerical studies presented in this chapter were concerning with the strengthening and repairing of non-prismatic beams, especially dapped end beams and haunched beams. The most popular material used for strengthening was CFRP on the other hand, the available studies in the literature review that have dealt with stepped beams are still limited. In addition, the past researches did not

provide data about using cotton in strengthening of RC members as a wide provided in local markets. Therefore, this research represents an attempt for studying the behavior of stepped beam. Different variables will be considered in this study to investigate their effects on the behavior of such members. Also, cotton belt strips is suggested as a new material used for strengthening stepped beams.

CHAPTER THREE
EXPERIMENTAL WORK

3.1 General

The main objective of this study is to investigate the behavior of reinforced concrete stepped beams improved by webbing and CFRP strip. A description of the program that explores the experimental variables, details of test specimens, and strengthening schemes are presented in this chapter. The properties of the constituent materials used in this study are tabulated. However, the preparation for test samples is presented in details.

3.2 Materials

The general description and specifications for the materials used in the testing program are listed below.

3.2.1 Cement

Portland cement (Type II) used throughout this study. They were stored in a dry place to avoid exposure to unwanted weather conditions. The results of the chemical analysis and the results of the physical tests for the cement is used are given in Table 3.1and Table 3.2, respectively. These are in accordance with Iraqi standard No. 5/1984 (Specification, 1984b).

3.2.2 Fine Aggregate

The sand used in all concrete mixtures was a natural sand. The maximum grain size is 4.75 mm and the modulus of fineness is 2.51. Laboratory tests for sand have been carried out according to the Iraqi

specifications No. 45/1984(Specification, 1984a). The results of these tests have been listed in Table 3.3.

3.2.3 Coarse Aggregate

In this study, natural gravel was used in concrete mix with grading satisfied to the limits of Iraqi standard No.45/1984 (Specification, 1984a) for graded gravel with a maximum size of 10 mm. Some properties of aggregate are illustrated in Table 3.4 and Table 3.5.

Table 3.1 Chemical composition of the cement.

Compound composition	Chemical composition	Percentage by weight	Limits of IOS 5:1984
Lime	CaO	62.00	_
Silica	SiO_2	21.00	_
Alumina	Al_2O_3	4.55	_
Iron Oxide	Fe_2O_3	3.14	_
Magnesia	MgO	2.77	<5
Sulfate	SO_3	2.10	<2.8
Loss on Ignition	L.O.I	3.11	<4
Insoluble residue	I.R	0.8	<1.5
Lime saturation factor	L.S.F	0.95	0.66-1.02
Main Compounds (Bogue's equation) percentage by weight of cement			
Tri Calcium Silicate (C_3S)	48.10		
Di Calcium Silicate (C_2S)	20.82		
Tri Calcium Aluminate (C_3A)	8.16		
Tetra Calcium Alumina Ferrite (C_4AF)	9.18		

Table 3.2 Physical properties of the cement.

Physical Properties	Test result	Limit of IOS 5:1984
Fineness Using Blaine Air Permeability Apparatus (m^2/kg)	310	$\geq$230
Setting time using Vicat's Instruments Initial (hrs: min.) Final (hrs: min)	 2:00 3:50	 $\geq$ 45min $\leq$10 hrs
Soundness Using Autoclave Method	0.21	<0.8
Compressive Strength 3 days (MPa) 7 days (MPa)	 20.0 28.9	 $\geq$15 $\geq$23

Table 3.3 Grading of the fine aggregate.

| No. | Sieve size (mm) | % Passing by weight | |
		Fine aggregate	Limits of IOS No. 45/1984-Zone2
1	10	100	100
2	4.75	100	90-100
3	2.36	94	75-100
4	1.18	82	55-90
5	0.60	50	35-59
6	0.30	15	8-30
7	0.15	8	0-10

Table 3.4 Grading of the coarse aggregate.

| No. | Sieve size (mm) | Passing (%) by weight | |
		Coarse aggregate	Limits of IOS No.45/1984
1	12	100	100
2	10	98	90-100
3	4.75	20	0-25
4	2.36	3	0-5

Table 3.5 Properties of the coarse aggregate.

Physical properties	Test results	Limits of IOS No.45/1984
Specific gravity	2.66	-
Sulfate content (SO_3)	0.077%	$\leq 0.1\%$
Chloride content (Cl)	0.094 %	$\leq 0.1\%$
Absorption	0.80%	-
Loose bulk density kg/m^3	1500	-

3.2.4 Silica Fume

Natural pozzolanic materials have become an important source in the production of essential materials for high-performance concrete mixtures, these including fine silica and fly ash. But micro-silica is more effective than fly ash for producing UHPC in mixtures which is commercially called silica fume or micro-silica (Tu'ma & Aziz, 2019). It

is available in local markets in bags of 20 kg, as shown in Figure 3.1. Fine silica granules are less than 0.1 micron and their chemical composition contains (Sio_2). This type of silica was used in the present work and it conforms to ASTM C 1240-04(ASTM, 2004). The chemical composition of silica fume used in this study presented in Table 3.6, which provided by manufacture.

Table 3.6 Chemical composition of silica fume.

Compound composition	Chemical composition	Oxide Content (%)	Limit of Specification Requirement ASTM C 1240-04
Lime	Cao	0.5	
Iron Oxide	Fe2O3	1.4	
Alumina	Al2O3	0.5	
Silica	Sio2	92.1	85 (min)
Magnesia	Mgo	0.3	
Sulphate	SO3	0.1	
Potassium Oxide	K2O	0.7	
Sodium Oxide	Na2O	0.3	
Loss on Ignition	L.O.I	2.8	6 (max)

Figure 3.1 Silica fume.

3.2.5 Water

Reverse osmosis (R.O.) water was used for mixing all concrete specimens and also for curing purpose.

3.2.6 Superplasticizer

One of the changes of producing a high-performance concrete mixture is to lower the water content, which is make difficult to mix. Therefore, it is necessary to add suitable plasticizers, highly effective in compensating for low water content. In the present work, a superplasticizer, type HyperPlast PC260 is used (see Figure 3.2). This type of plasticizer conforms to ASTM C494-99 A and G (ASTM, 1999). This plasticizer is chloride-free, based on poly carboxyl polymer with a long chain designed specially to enable water to perform more effectively, directly affecting the increased operability of concrete and giving it adequate flow through confused. The technical specifications for this type of plasticizer are described in Table 3.7.

Table 3.7 Technical Description of PC 260.

Chemical base	Modified poly carboxylates based polymer
Appearance /colors	Light yellow liquid
Freezing point	-7°C approximately
Specific gravity @25°C	1.1±0.02
Air entrainment	Typically less than 2% additional air is entrained above control mix at usual dosage
Dosage	0.5 to 4 liter per 100 kg of binder
Storage condition /shelf life	12 months if stored at temperatures between 2°C and 50°C

Figure 3.2 Hyperplast PC260.

3.2.7 Webbing

Webbing is a sturdy fabric woven as a flat ribbon or tube varying in width and fiber, it is often used instead of rope. Originally, it is made of cotton or linen, most of the modern belts are made of synthetic fibers such as nylon, polypropylene or polyester. It is a versatile component, with low cost and high tensile strength used in automobile safety, towing, load insurance and many other areas. The type used in the present study is cotton belt. It is available in the local market with different sizes. It is a very cheap materials. The dimensions of cotton belt used are 75 mm width with 3 mm thick as shown in Figure 3.3. Table 3.8 showed the properties of webbing (Dhiaa,2021) and (Meruane et al,2015) for cotton belt.

Table 3.8 webbing properties (Dhiaa,2021), (Meruane et al,2015)

Length (mm)/roll	Width (mm)	Thickness (mm)	Load (kN)	Ultimate Tensile Stress (MPa) (average of three samples)	Young's Modulus for cotton belt (GPa)
7500	60	3	52.2	290	5.5-12.6

Figure 3.3 Cotton belt.

3.2.8 Carbon Fiber Reinforced Polymer (CFRP)

SikaWrap®-300 C/60 carbon fiber fabric was used to externally reinforce the reinforced concrete beams. When loaded in tension, it shows no plastic behavior before rupture. The tensile behavior of CFRP is characterized as a linearly elastic stress–strain relationship up to failure. The failure of CFRP is sudden and potentially catastrophic. Mechanical properties of CFRP sheets are shown in Table 3.9 as provided by manufacturing specifications (Mohy et al., 2013).

Table 3.9 Mechanical properties of CFRP material.

Criteria	CFRP sheets
Tensile strength (MPa)	3500
Modulus of elasticity (GPa)	230
Failure strain (%)	1.50
Thickness (mm)	0.13

3.2.9 Bonding Materials

Sikadur®-330 was used in this work to bind the webbing and CFRP. It is a two-components, solvent-free, moisture-tolerant, high strength, high modulus structural epoxy adhesive. The mixing ratio of the epoxy was four parts resin of component A (white paste) to one part hardener of component B (grey paste) by weight. Components of sikadur330 are shown in Figure 3.4 (Sika, 2017).

Figure 3.4 Sikadur330.

3.3 Steel Reinforcement

Deformed steel bars of 12 and 10 mm diameter were used for longitudinal reinforcement and deformed steel bars of 8 mm diameter are used for stirrups. Table 3.10 shows the properties of reinforcing bars used in this study. Figure 3.5 shows stress-strain curve of steel bar and Figure 3.6 shows the tensile strength of reinforcement test bars. Rebar's test was carried out according to the American Standard Specification for deformed and plain steel bars ASTM A615,2020 (Standard, 2020).

Table 3.10 Properties of reinforcing bars

Bar size (mm)	Test results			ASTM A615/A615M		
	Yield strength (N/mm^2)	Ultimate Strength (N/mm^2)	Elongation (%)	Yield strength (N/mm^2)	Ultimate Strength (N/mm^2)	Elongation (%)
8	423	527	29	419	525	28
10	488	610	16	420	550	9
12	562	665	15	420	550	9
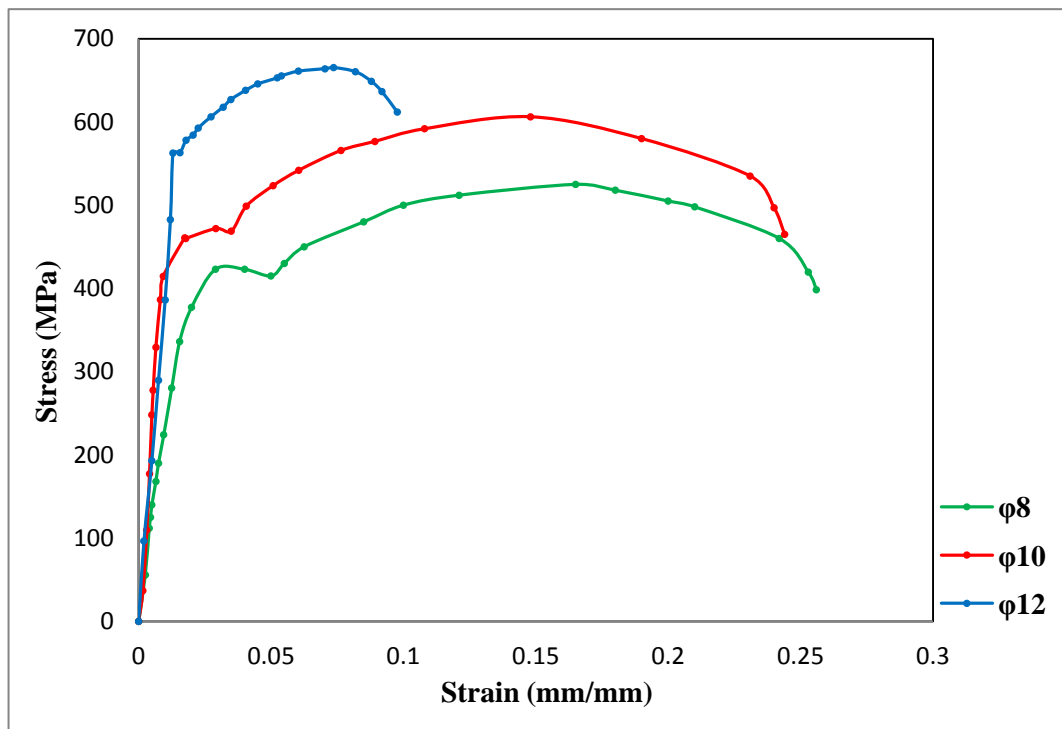
Figure 3.5 Stress-strain curve of steel bar
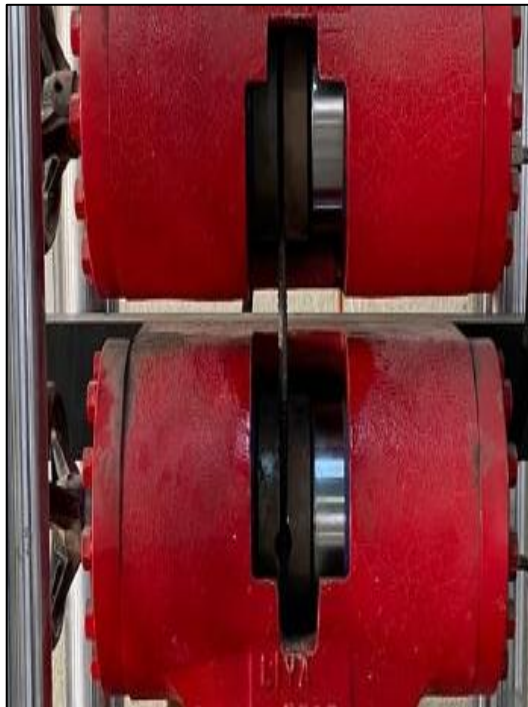
Figure 3.6 Tensile strength of reinforcement test bars.

3.4 Preparation of Test Specimens

3.4.1 Mix Design

Normal and high strength concrete mixtures were prepared in this study. For normal concrete mixture, the amount of concrete compositions with respect to weight of cement are 1:1.25:1.50, water to cement ratio 0.4. The average cylinder compressive strength obtained from this mixture was 40 MPa at 28 days while these ratios become1:1.25:1.5 for producing high strength concrete with 85 MPa at 28 days. Because the water to cement ratio is very low in high strength the mixture, the high range water reducer was used. Hyperplast PC260 superplasticizer with 1.8% of cement weight was added to concrete mix to improve the workability. Also, silica fume with 10% of cement weight was utilized as a supplementary pozzolonic material which was widely used in high strength mixture. Figure 3.7 shows the concrete mixer used in work.

Figure 3.7 Concrete mixer used in present study

3.5 Details of Test Specimens and Schemes

A total of fourteen reinforced stepped beams were prepared for test. The beams were divided into two series; unstrengthened and strengthened specimens. The main variables were concrete compressive strength (40 and 85) MPa, strengthening materials (CFRP and cotton belt), and in term of steel configurations. The stepped beams were composed of two parts; lower and upper portion. The overlap region called stepped portion or stepped joint. The beam dimensions were the same of all specimens. The beam total length was 2300 ±3 mm with 2100±3 mm center to center span from the supports. The cross-section of lower and upper portions were (150×300) mm. While the stepped joint cross section dimensions were (150×450) mm as shown in Fig. 3.8. The flexural reinforcement of all beams 2Ø12 mm was used, while the steel compression was 2Ø10 mm used as stringer. The transverse reinforcement was Ø8 mm rebar as a closed stirrups spaced at 100 mm interval.

The stepped beams were separated into two groups; unstrengthened and strengthened specimens. The first group consisted of four specimens (N, H, Ni and Hi) which were unstrengthened specimens; in which Ni and Hi beams considered as reference beams. The details of specimens in this group are shown in Figure 3.8 and Figure 3.9. The second group consisted of eight specimens and these were strengthened externally. The specimens (Nw1, Hw1, Nw2, Nws2, Hws2 and Nw2s) were strengthened by using cotton belts, while specimens (Nc and Ncs) were strengthened by using CFRP. These beams were externally reinforced. The letter N meaning normal compressive strength with fc´=40 Mpa and H refer to the high strength concrete with fc´=85 Mpa.
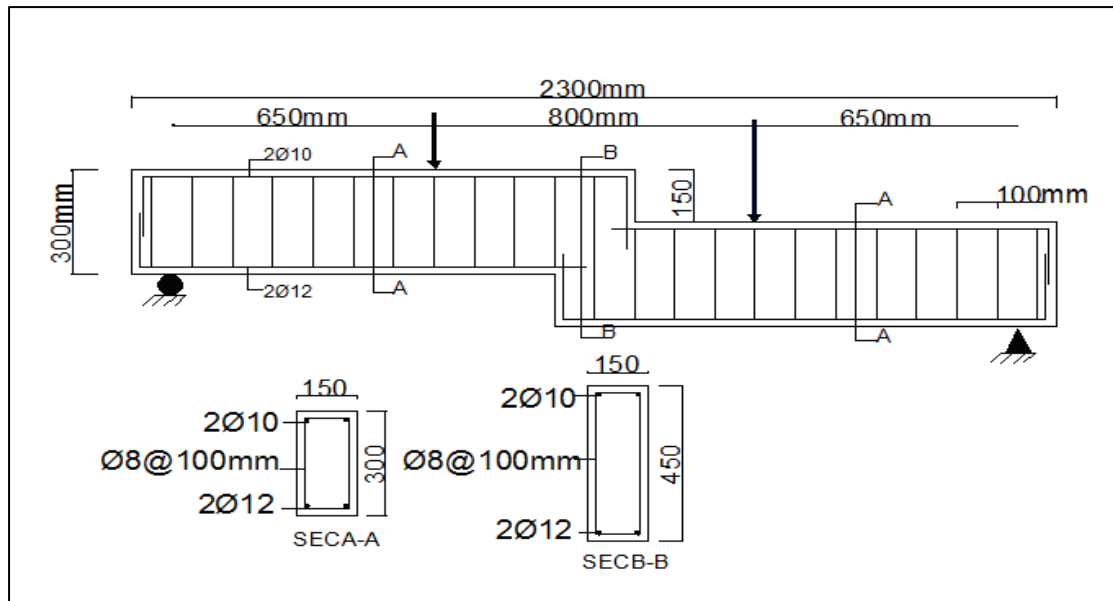
Figure 3.8 Details of beams N and H.
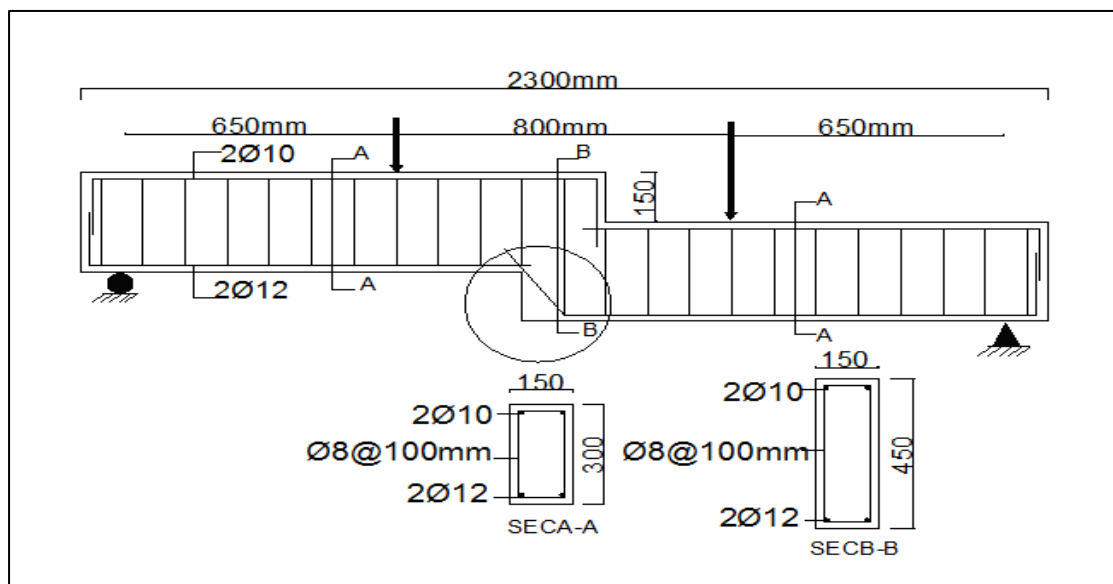
Figure 3.9 Details of beams Ni and Hi.

The beams Nw1 and Hw1 were strengthened by single layer of U-shape cotton belt at the centered region (between applied points). The specimen Nw2 was strengthened by using double layers of U-shape cotton belt. Figure 3.10 and Figure 3.11 show strengthening schemes of specimens.
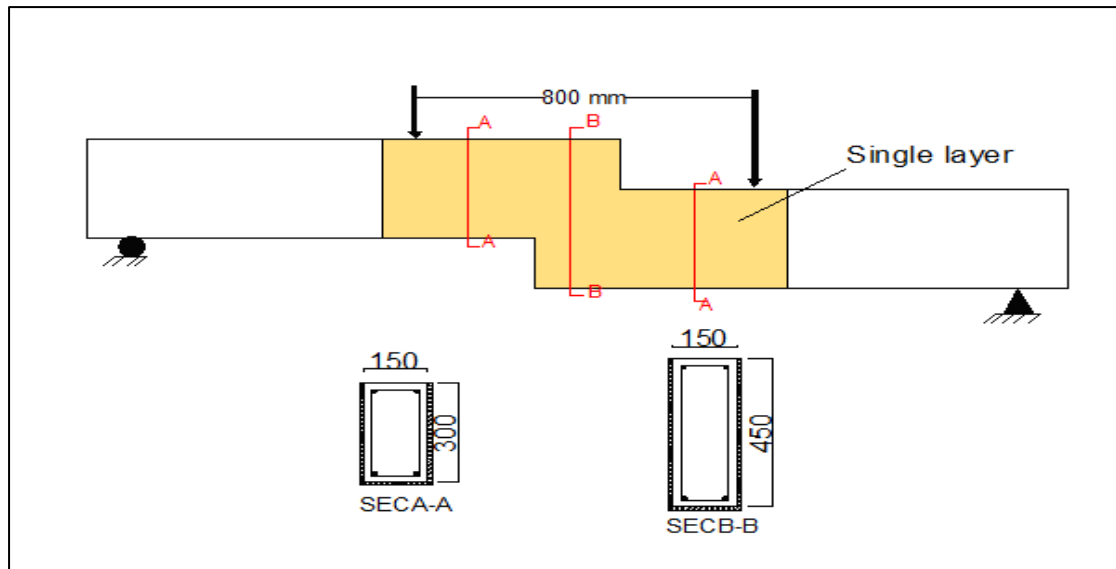
Figure 3.10 Details of beams Nw1 and Hw1.
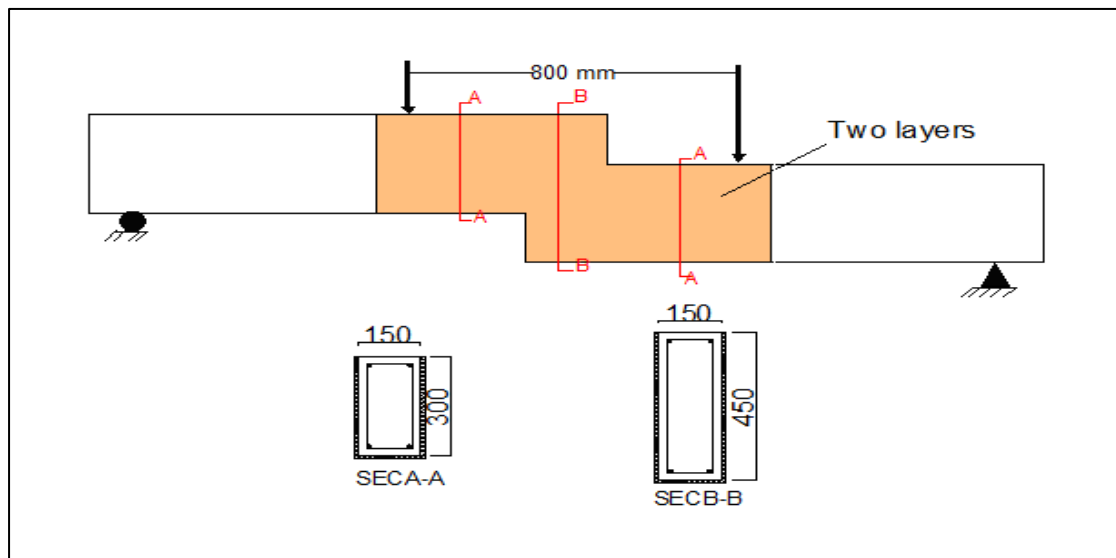
Figure 3.11 Details of beam Nw2 .

The beams Nws2 and Hws2 were strengthened by double layers of cotton belt at the region of applied load and stepped joint as shown in Figure 3.12. The beam Nw2s1 were strengthened by single layer of cotton belt at the region, double layers at the stepped joint and applied load regions as shown in Figure 3.13.
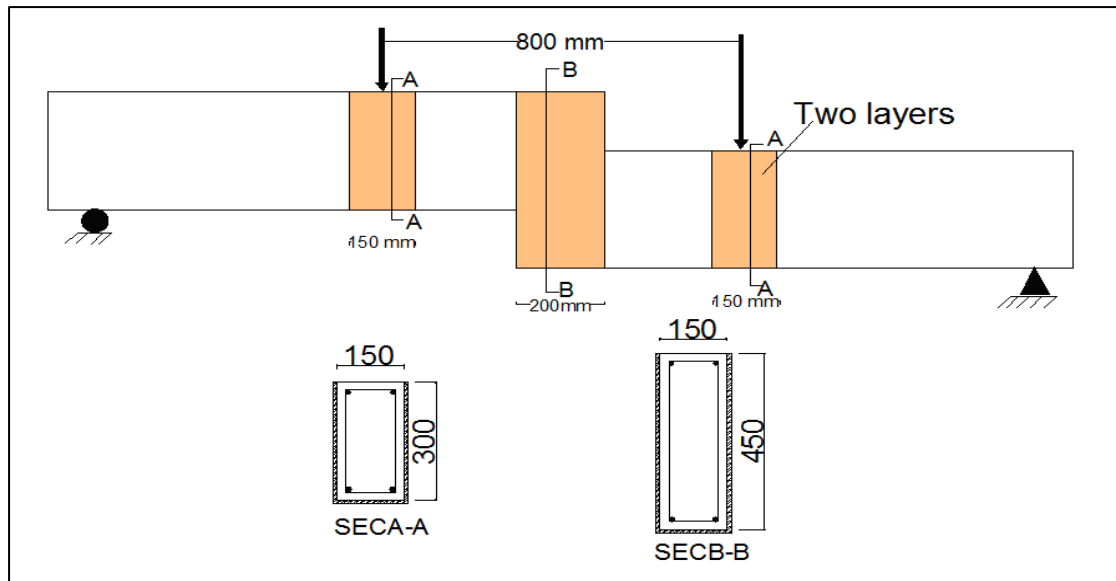
Figure 3.12 Details of beams Nws2 and Hws2.
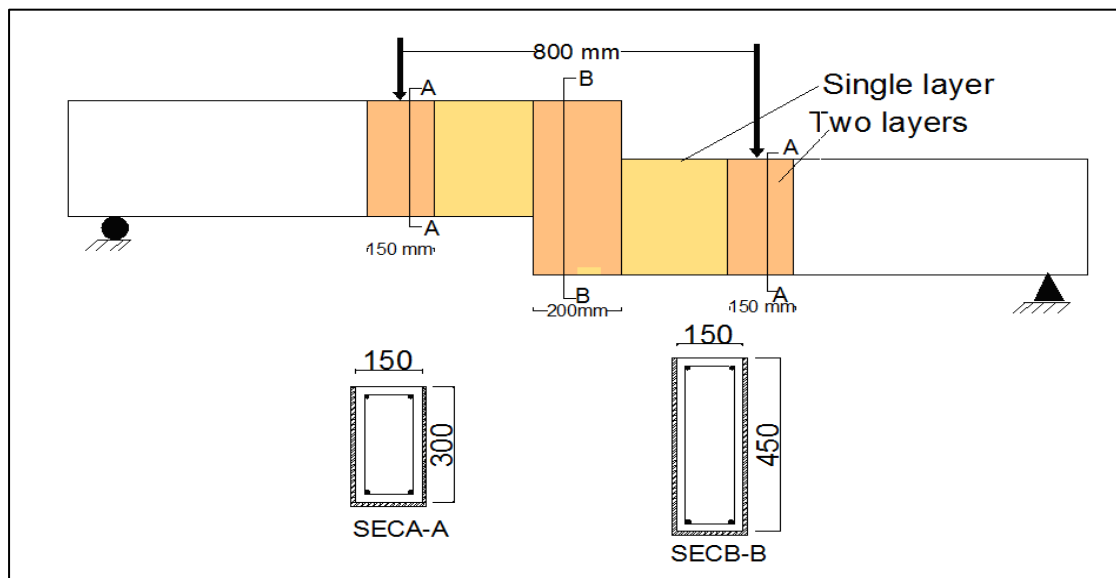
Figure 3.13 Details of beam Nw2s1.

The other two stepped beams were strengthened by CFRP sheet. The beam Nc was strengthened with CFRP sheet (U-shape continuous) at the middle region with length of 950 mm, while the beam Ncs was strengthened by using CFRP at the applied load and stepped joint regions as shown in Figure 3.15 and Figure 3.14.
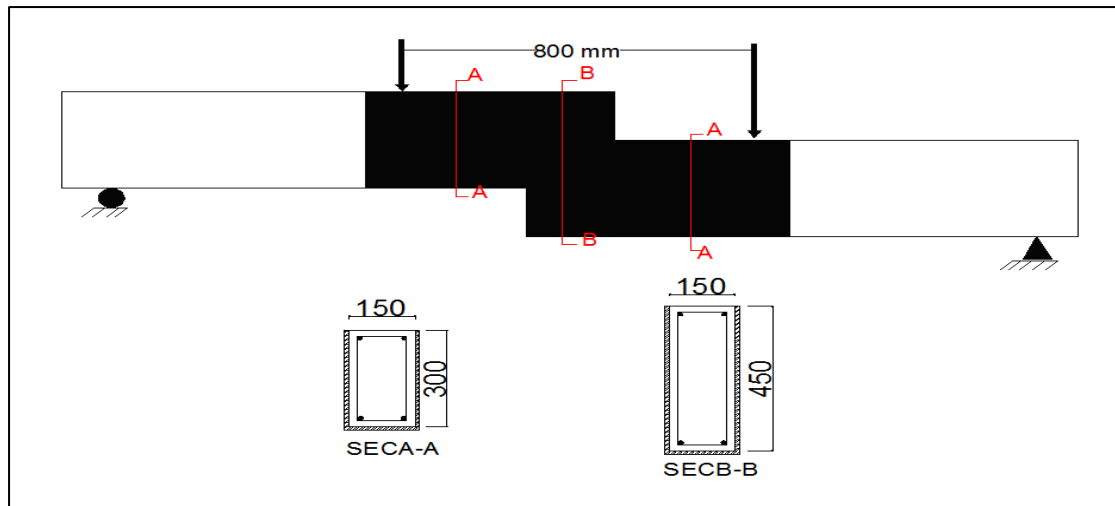
Figure 3.14 Details of beams Nc.
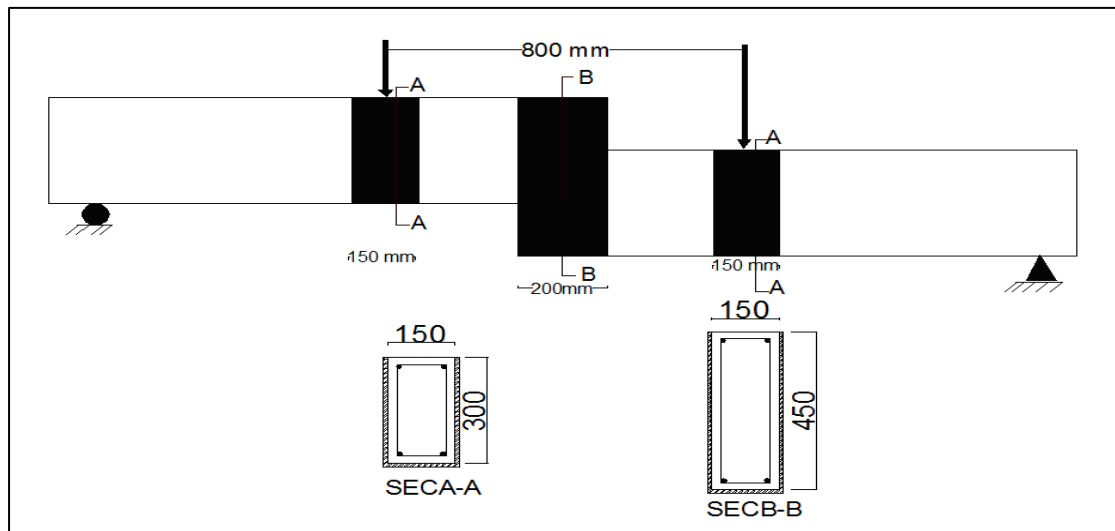
Figure 3.15 Details of beams Ncs.

The remaining two beams H-int and H-inc were internally strengthened by using different in term steel configurations. For this purpose the internal reinforcement beams was done using 8 mm rebar. The beam H-int was strengthened by using horizontal and vertical reinforcement spaced by (30 and 40) mm, respectively, while the beam H-inc was strengthened by horizontal, vertical, and inclined reinforcement spaced by (80, 75 and 50) mm respectively, Figure 3.16 and Figure 3.17 illustrate the internal steel distribution in the middle region of beams H-int and H-inc.
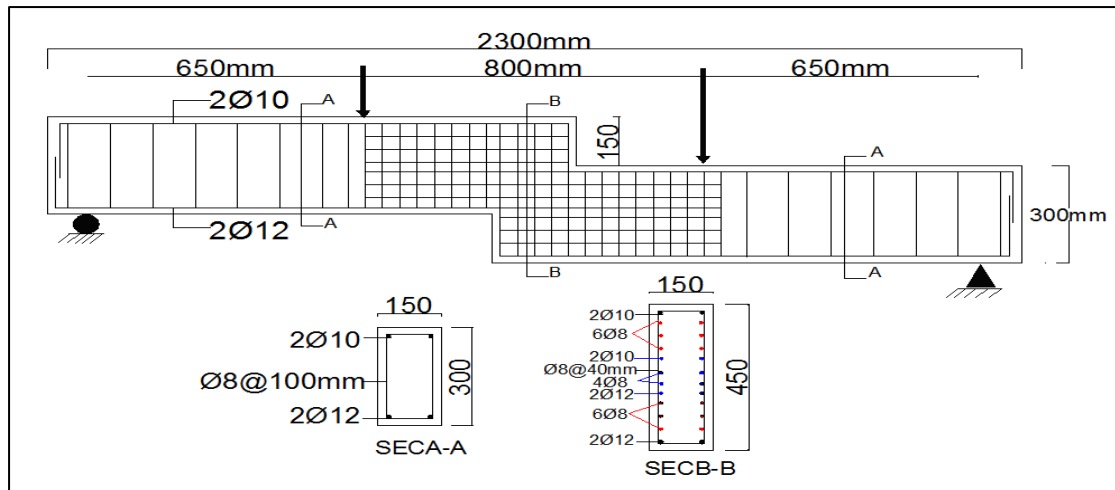
Figure 3.16 Details of beam H-int.
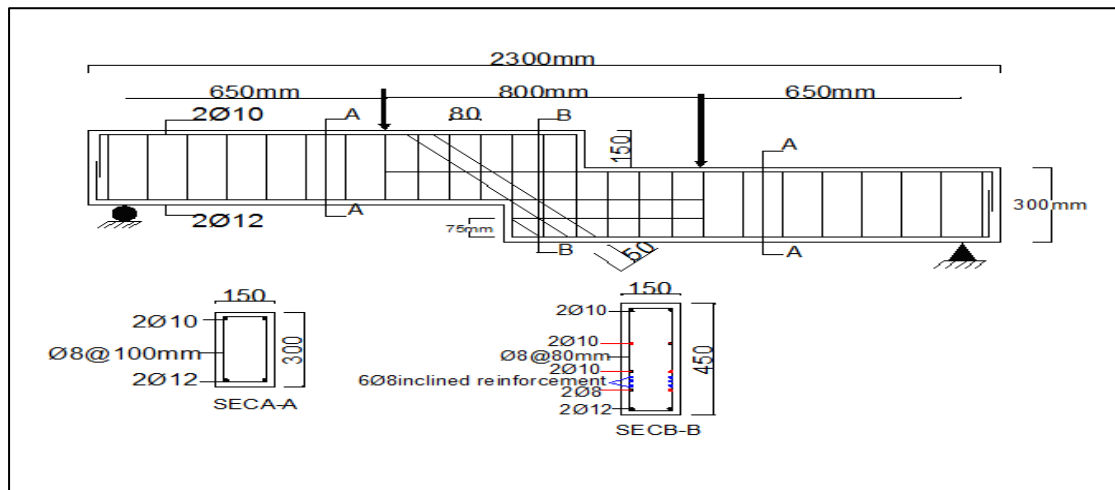
Figure 3.17 Details of beam H-inc.

3.6 Beam Molds

Wooden formwork was used to cast all concrete beams, as shown in Figure 3.18. All molds consist of a wooden base and four movable sides connected to base with screws and nails. The length of mold was 2300 mm for all beams, the length of specimens depending on previous studies. The previous studies did not address the ratio of the length of the concrete beam (L)to the depth of the section (d) due to the fact that the concrete beam contains a stepped joint. The beam cross-section was (150 x 300) mm ,while it was (150 × 450) mm for the stepped joint region.

Figure 3.18 Beam molds.

The steel bar that utilized in the all specimens was 2 Ø10 mm in the compression zone, while the steel bar that was used in the tension zone was 2 Ø 12mm. The transverse reinforcement was Ø8@100 mm. The work was done by two technicians men according to the specifications, as shown Figure 3.19. The specimens were cast in a horizontal direction because the difficulty of fix the specimens in the vertical direction during the casting.

a- Specimens Ni and Hi

b- Specimens N and H

c- Specimen H-int

Figure 3.19 Steel reinforcement details.

3.7 Mixing Procedure

3.7.1 Normal Strength Concrete

The mixture was mixed in the structural laboratory at the college of Engineering in University of Misan. All quantities were weighed and packed in a clean container before mixing. Saturated and dry surface gravel, sand and cement were mixed in a rotary mixer for 4 to 5 minutes. Water was added to the mix and all the materials were remixed for 2 minutes. Concrete was poured into the molds in two layers, each layer was compacted by electrical vibrator (internal vibrator) to shake the mix and consolidate it into the molds.

3.7.2 High Strength Concrete

The mix proportions of the ingredients by dry weights were [1 cement: 1.25 sand: 1.5 gravel]. The water cement ratio (w/c) was 25%. The ratios of superplasticizer and silica fume to cement weight added were 1.6% and 10%, respectively to give a cube compressive strength about 85 MPa at the age of 28 days. After samples preparation, the mixing process was started by adding the desired quantities of cement and the desired quantity of silica fume and mixed in dry state then a required quantity of sand and gravel was added. This operation was continued to two minutes for ensure that silica fume powder was thoroughly dispersed between the sand particles. Then the superplasticizer was dissolved in water and the solution of water with superplasticizer was added to the rotary mixer gradually and the whole mix ingredients were mixed for a sufficient time after that the concrete mix was poured in molds and left for 24h. At the end of 24h, the specimen was removed from the mold and cured by covering it with wetted clothes as shown in Figure 3.20.

Figure 3.20 Pouring and processing beams.

3.8 Mechanical Properties of Concrete

During casting, nine 150 ₓ 150 ₓ 150 mm cubes, six (100×200) mm cylinders and three (100 x 100x 500) mm prisms for each type of concrete were made. The control specimens were compacted and cured under the conditions of stepped beams as shown in Figure 3.21. All molds were prepared, cleaned, and lubricated before casting.

Figure 3.21 Specimens of hard concrete tests (cubes, cylinders and prism).

3.8.1 Compressive Strength

The cube compressive strength of concrete was obtained by testing cubes according to BS1881: Part 16: 1983 (BS 1881, 1989). The test was conducting by using 2000 kN compression testing machine at the laboratory of constructer material in the Department of Civil Engineering department. The test results are presented. The average compressive strength obtained of normal and high strength concrete are 45.68MPa and 85.82 MPa, respectively. The test results are presented in Table 3.11. Shown in Figure 3.22

Figure 3.22 Compressive strength test.

Table 3.11 Compressive strength results of normal and high strength concrete

Age	Compressive strength of normal concrete (MPa)	Compressive strength of high concrete (MPa)
7 days	37.4	75.2
	37.6	76.0
	37.9	76.3
28 days	45.6	85.9
	46.0	86.5
	45.2	85.8
	45.5	86.2
	45.7	85.3
	46.1	85.2
Average of 28 days	45.7±0.27	85.8±0.42

3.8.2 Split Tensile Strength

ASTM- C496 (C496, 2006) has been adopted to check split tensile strength of concrete cylindrical (100 ×200) mm. This test was done at the College of Engineering in the University of Misan by using compression testing machine with a capacity of 2000 kN as shown in Figure 3.23. The test results are presented in Table 3.12. The split tensile strength of concrete was calculated by using the following formula 3.1

$$F_t = \frac{2p}{\pi D l}$$ 3.1)

where ; F_t: is tensile strength (MPa) ; p :is ultimate failure load (N); D:is diameter of cylinder specimen (mm); and l: is length of cylinder specimen (mm).

Figure 3.23 Split tensile strength test.

Table 3.12 Results of splitting tensile strength.

	Split tensile strength (MPa)	
	Normal strength concrete	High strength concrete
	2.7	4.7
	2.6	4.8
	2.7	5.2
	2.8	4.8
	2.6	5.3
	2.8	4.7
Average	2.7±0.07	4.9±0.22

3.8.3 Flexural Strength Test

ASTM-C78 (C78, 2002) was adopted to check the bending strength of concrete by using prism samples (100 × 100 ×500) mm for testing. This test was conducted at the college of Engineering at the University of Misan by using flexural machine with a capacity (50 kN) as shown in Figure 3.24. The test results are presented in Table 3.13. The following equation 3.2 is used to calculate the bending strength:

$$F_r = \frac{3pl}{2bd^2}$$ 3.2)

where; F_r: is modulus of rupture (MPa); p: is maximum applied load (N) ;l: is span length (mm) ; b: is average width of the specimen (mm); and d: is average depth of specimen (mm).

Table 3.13 Flexural strength result.

	Flexural strength (MPa)	
	Normal strength concrete	High strength concrete
	4.5	8.8
	4.4	8.6
	4.5	8.4
Average	4.5±0.04	8.6±0.14
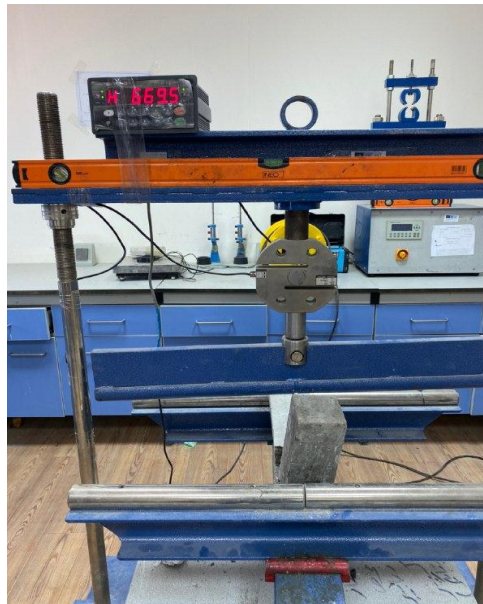
Figure 3.24 Flexural strength test.

3.9 Installation of Strengthening System

Before adhering of CFRP and webbing (belt strip) to the surface of concrete for strengthening purpose, preparation of the surface were done as a preliminary stage to ensure a high quality bond. These include preparation the substrate of concrete, ensuring the flatness of concrete surface for adhering strengthening system and setting out the strengthening material in an exact locations. The preparation of the

concrete substrate include removal all dirt and cement laitance. A layer of concrete surface of (0.5 – 1.0) mm was removed to expose coarse aggregate by using grinding tool. Further, any materials and dust should be removed by using water jet. The surface of concrete to which the strengthening material is bonded should be sufficiently flatness to avoiding developing any out of plane stresses. ACI 440.2 (440.2R, 2017) in 2017 limited the surface curvature per meter should not be greater than 5 mm. To ensure the strengthening materials placed in stepped joint and alignment, the location of strengthening strips or sheet must be marked before application. The bonding of strengthening materials (CFRP and webbing) on to the surface of concrete includes the following steps:

1. The primer should be applied to the concrete substrate and permitted to become to a tacky state.

2. Distributing very fine sand on the concrete surface to enhance the roughness of concrete substrate .

3. Mixing two components (A and B) of adhering material according to the manufacture guidelines, Sikadur 330 was used in this study.

4. Thin layer of adhesive material was used in adhering bonding strengthening system to fill all voids in the substrate.

5. Also, thin layer of adhering material should be applied in both concert substrate and strengthening strips.

6. The strengthening strip should be placed on the stepped joint and rolled to remove entrapped air by using hard rubber roller.

In the case of multi layers of strengthening strips which are used, the second layer must be applied at time of the adhesive resin in the previous layer which should not have hardened. Figure 3.25 shows the details of preparation and installation of strengthening system. In addition Figure 3.26 Strengthening of specimens.

a- Surface grinding

b- Cleaning the surface of concrete

c-Weighing primer

d- Mix primer

e- Applied primer to concrete surface

f- Distribute very fine sand

g- Saturated webbing with epoxy

h- applied the webbing on
   the concrete surface

Figure 3.25 Preparing and setting webbing and CFRP.
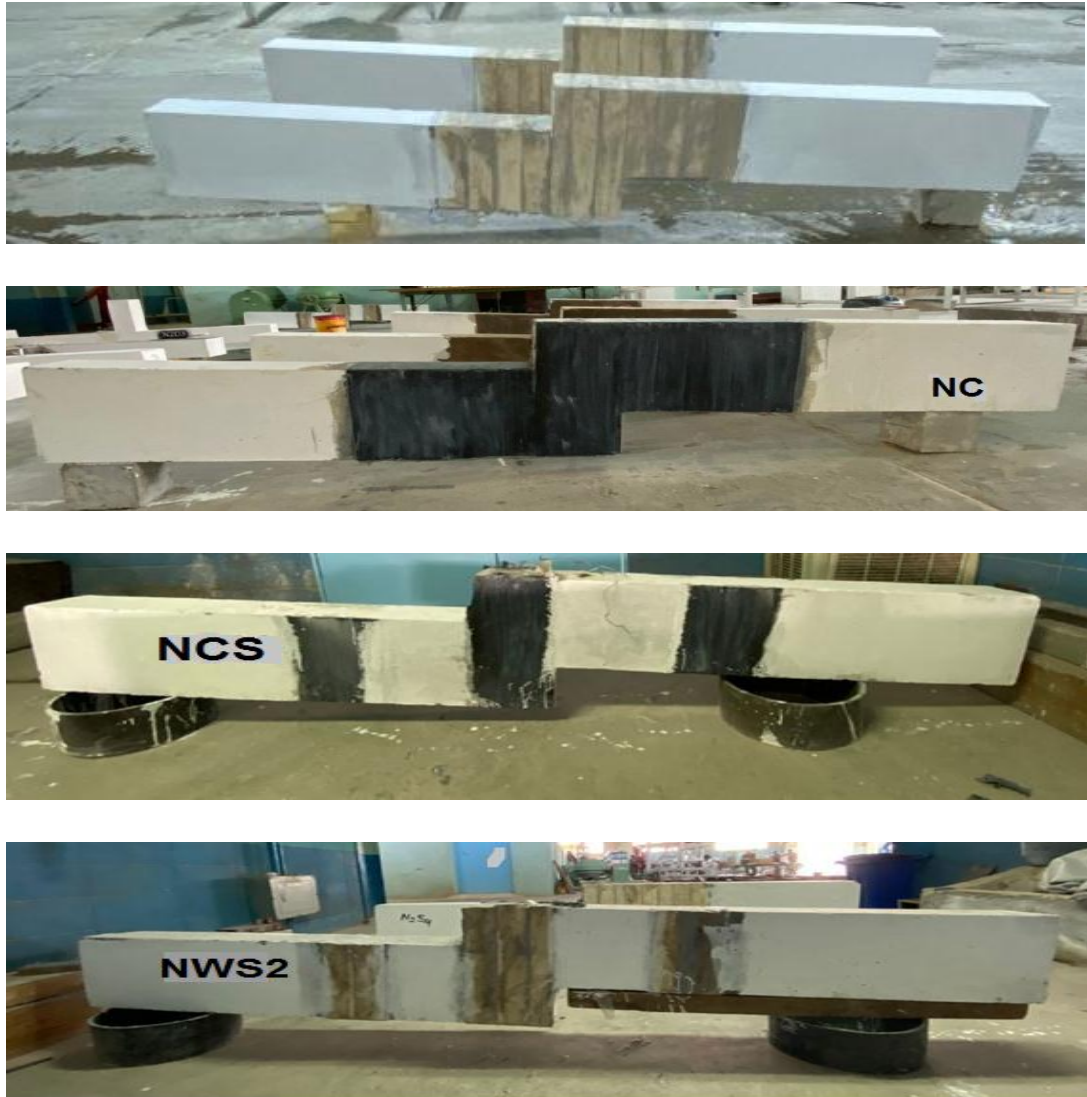
Figure 3.26 Strengthening of specimens.

3.10 Strain Gages

One (30 mm) strain gauges were attached at the top of each beam before the test was placed in the compression zone in the stepped region . It was connected to data acquisition device (data logger consists of 16 channels supplied with DATACOMM software for PC data acquisition) to obtain strain reading at each load increment as shown in Figure 3.28. The strain gauge was bonded by using CN-E cyanoacrylate adhesive to the previously treated surface of the stepped beam. See Figure 3.27.

(a) PFL-30-11-3L strain gage   (b) Adhesive materials

Figure 3.27 Strain gauges attached to the beam.

3.10.1 Data Acquisition System

The data obtaining system includes a personal computer, a strain indicator called the data logger and its function is receiving data from a set of strain gauges that adhesion on the beam, the name of data logger is GEODATALOG 30-WF6016 and its properties are 16 channels data acquisition unit. 110-240 V, 50-60 Hz, 1ph supplied complete with DATACOMM software for PC data acquisition, as shown in Figure 3.28.
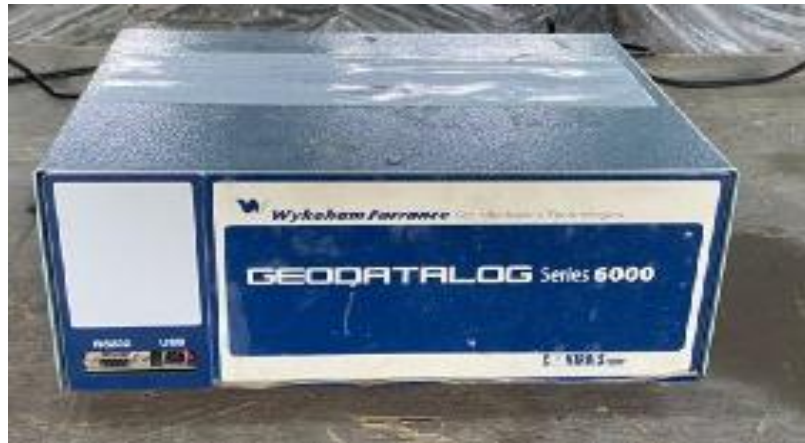
Figure 3.28 The used data logger.

3.10.2 Deflection Measurement

The mid-span deflection of each beam was measured by using a dial gauge with a magnetic base. The accuracy of the dial gauge was 0.01 mm. See Figure 3.29. The dial gauge was placed at the center of span.

Figure 3.29 Used dial gauge.

3.11 Test Procedure

All beam samples were tested by the universal testing machine of 60 tons capacity as shown in Figure 3.30. This test done in the laboratory of the Technical Institute of Amarah. All samples were cleaned and painted

with white paint prior testing to demonstrate the propagation of cracks. Two concentrated loads were applied through a steel loading plate over a thin rubber strip which was used to achieve a uniform contact. The initial readings of the deflection dial gauge the strain gauge were recorded at the beginning of the test. In all tests, the load was applied and readings of deflection, strain and load were recorded in each increment. The load was gradually increased until failure.

Figure 3.30 Test arrangement.

CHAPTER FOUR
RESULTS AND DISCUSSIONS

4.1 General

The main objective of the current research work is to investigate the structural behavior of reinforced concrete stepped beams externally strengthened with cotton belts and carbon fibers reinforced polymer (CFRP) sheets. In this chapter, tests results for experimental program are presented to investigate the influence of the experimental variables on behavior of beams specimens. The variables include, compressive strength normal and high strength, internal reinforcement, number of cotton belts layers (1 layer or 2 layers), and external strengthened with CFRP sheets.

In the current study, fourteen reinforced concrete beams were tested under two point loads until failure. As for the variable of strengthening, seven RC beams were strengthened with cotton belts and two beams is strengthened with CFRP sheets, while the variable of reinforcement, included two RC beams with different schemes of internal reinforcing as well as, two beams specimens are used as control beams for comparisons. All beams possess the same length and cross sectional area. They are identically reinforced as described in chapter three. Test results are analyzed via cracking load, ultimate load, failure modes, ductility, toughness, mid span deflection, and strains distribution.

4.2 Load - Deflection Response

Figure 4.1shows the relationship of load vs deflection of references stepped beam (Ni and Hi). From this figure, it is observed that the relations is linearly proportion. This continue till the appearance of crack

at the mid span region (between the applied load). With increasing of applied load, more new cracks appeared, and the response of the beams are changed. The relations of load vs deflection displayed nonlinear behavior of the beams response. After that, with further increased of the load, one of the cracks become widen and extended more than of the other cracks causing the collapse of the beam. At this stage, the load – deflection curves become more flat and its approached to the horizontal line.

The load – deflection curve of specimens N and H is shown in Figure 4.1The specimens N and H have the same reinforcement of the control specimens Ni and Hi but the details of reinforcement at the stepped joint are different as shown in Figure 3.8 and Figure 3.9. These beams exhibited a reduction of the ultimate load and deflection compared with the reference (Ni and Hi).

The beam N has lower ultimate load and deflection of Ni. The lowering ratio of ultimate load and deflection were 65.9% and 27.34% compared with Ni, respectively. While, the lowering ratio of ultimate load and deflection were 47.33% and 4.10% compared with that of Hi, respectively. The cause make the beams N and H have lower responses is due to change in reinforcement from vertical at beams (N and H) to inclination at beams (Ni and Hi) at the tensile region , the inclination reinforcement perpendicular to the crack and restriction.

For the specimens (H-int and H-inc) which is made of high concrete strength with internal strengthening, (H-int with intense reinforcement at stepped joint and H-inc with inclination reinforcement at stepped joint), for beam H-int the increasing ratio in ultimate load and deflection are 277.2% and 210% respectively. Also, for beam H-inc the increasing ratio for both ultimate load and deflection are 253.84% and 222.30% respectively, compared with that of Hi. This improvement in

strength for beams H-int and H-inc is due to the presence of intense and inclination reinforcement in the stepped joint.

The externally strengthened stepped beams (Nw1 and Hw1) which have the same strengthening are strengthened with one layer of the cotton belt. For the specimen Nw1which is made of normal concrete strength showed an increase in deflection and ultimate load of 248% and 41.98% compared to the reference beam Ni, respectively. The beam Hw1is made of high concrete strength, it is observed that an increase in ultimate load and deflection by 120.5% and 34.66% compared to the reference beam Hi, respectively. Also, the ultimate load of beam Hw1is higher than Nw1 by 67.3%. This increasing is due to the different properties of high strength concrete in terms of higher compressive strength and higher tensile strength than normal concrete strength.

For the specimen Nws2 which is made of normal concrete strength and strengthened with two layers of cotton belt at stepped joint and under the load region exhibited higher ultimate load and maximum deflection compared with the reference beam. The increasing ratios were 17.4% and 26.8% for ultimate load and deflection, respectively. The same note was observed for specimen Hws2 which was made of high strength concrete. The increasing ratios with respect to the reference beam for ultimate load and maximum deflection were 80.25% and 70.3%, respectively.

Also, a significant increasing in ultimate load and deflection had been observed for specimen Nw2 which was strengthened by double layers of cotton belt placed along the middle span region. The increasing ratios compared with reference beam were 71.82% and 34.4% for both load and deflection, respectively.

When making comparison between the specimen Nw2 and Nw1, the ultimate load of specimen Nw2 was higher than that of Nw1 by 21%.

This indicates that using two layers of strengthening stepped beam is effective.

For the beam Nw2s1 which was made of normal concrete strength and strengthened by two layers of cotton belt at stepped joint and under the load region recorded an increase in deflection and ultimate load by 81.15% and 50.5 % compared to reference beam, respectively. For beams strengthened by two layers of the cotton belt, due to the presence of the second layer of the cotton belt, the beams showed less deflection than those with one layer strengthened beams. This improvement in strength was attributed to the presence of the cotton belt and which led to the conversion of the crack from several widely spaced and large width cracks to many more closed spaced narrower cracks.

For the specimens Nc and Ncs which are made of normal concrete strength and strengthened with one layer of CFRP at stepped joint and under the load region. The Nc beam achieved an increase in deflection and ultimate load by 94.74% and 62.15% compared to the reference beam Ni, respectively. Also, increasing of ultimate load and deflection for specimen Ncs, the increasing ratios of deflection and ultimate load compared with control beam are 15.9% and 22.9%, respectively. The CFRP sheet's presence is attributed to this strength increase, another advantage is the presence of CFRP, shifting the crack to several more closed spaced cracks and reducing the beam's deflection. The beams strengthened with continuous U- configuration (Nw1, Nw2, Hw1 and Nc) showed a significantly higher increase in ultimate load in comparison with beams strengthened with vertical isolated strip of cotton belt and CFRP. The presence of strengthening of the strip configuration in the beam led to the extension of the crack between the strips and prevented the crack from extending, while the continuous u-configuration in the middle region delayed the crack's appearance and prevented its

appearance. The reinforced stepped beams strengthened with cotton belt and CFRP sheets show lower deflections at the same loads from those of unstrengthened beam due to the presence of cotton belt and CFRP sheets. Figure 4.1shows the vertical load versus mid-span deflection for all beams. Table 4.1shows the deflection and ultimate load for all beams.
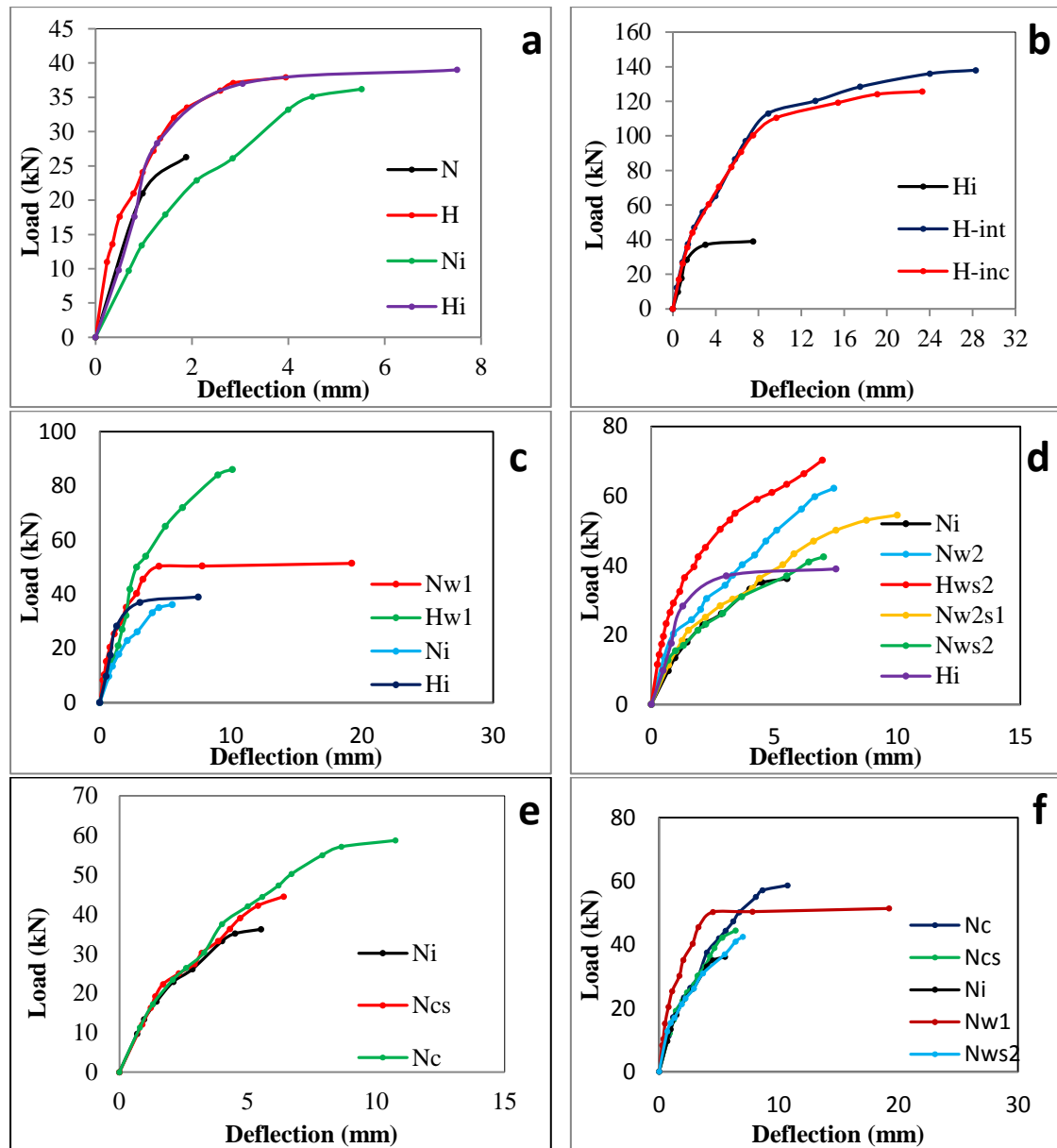
Figure 4.1 Vertical load versus mid-span deflection for
a- Unstrengthened beams, b- Internal strengthening beams, c-External strengthening beams by one layer of cotton belt ,d – External strengthening beams by two layer of cotton belt, e- External strengthening beams by CFRP, f-   External strengthening beams by cotton belt and CFRP.
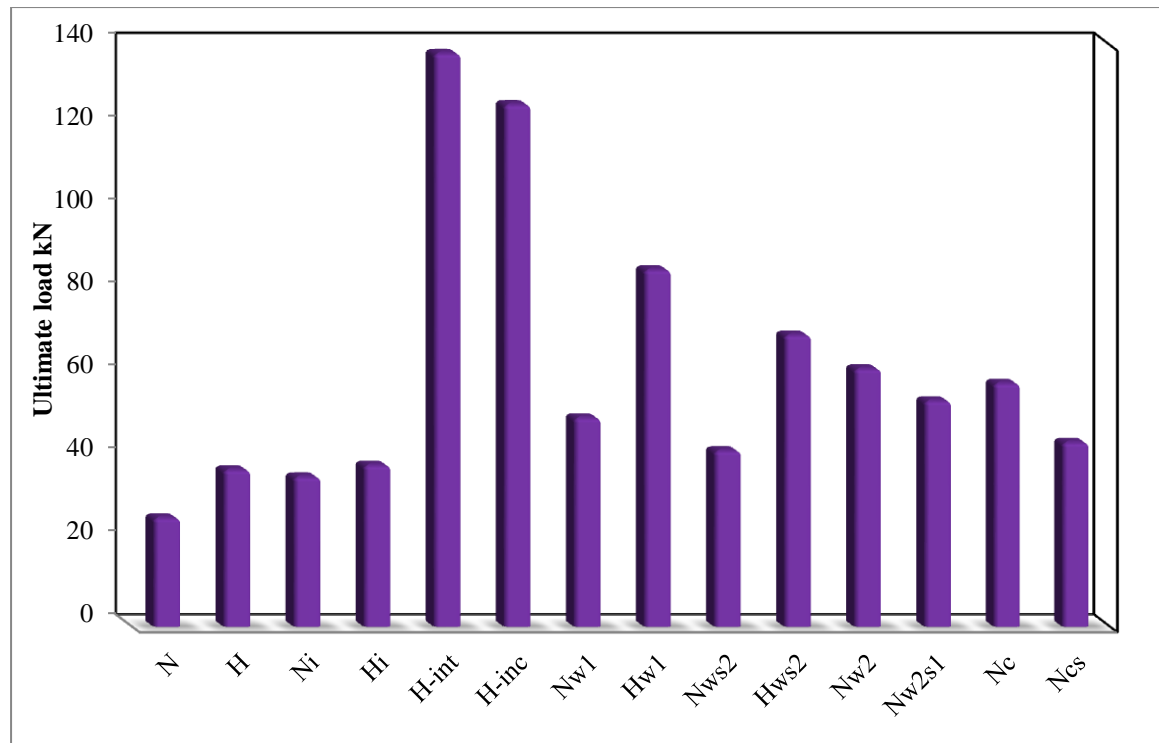
Figure 4.2 Ultimate load capacity of all tested beams.

Table 4.1 Deflection and ultimate load for all beams

Beam remark	Deflection mm	Increasing ratio of deflection %	Ultimate load kN	Increasing ratio of ultimate load %
Normal strength concrete				
Ni	5.52	-	36.2	-
N	1.88	-65.94	26.3	-27.34
Nws2	7.00	26.80	42.5	17.40
Nw1	19.22	248.18	51.4	41.98
Nw2	7.42	34.40	62.2	71.82
Nw2s1	10.00	81.15	54.5	50.50
Ncs	6.40	15.90	44.5	22.90
Nc	10.75	94.74	58.7	62.15
High strength concrete				
Hi	7.5	-	39	-
H	3.95	-47.33	37.4	-4.10
H-int	28.29	277.2	138	253.84
H-inc	23.31	210.8	125.7	222.30
Hws2	6.95	-7.33	70.3	80.25
Hw1	10.10	34.66	86	120.5

4.3 Initial Stiffness

The initial stiffness is the slope of the first part of the load-deflection curve. It is calculated by dividing the yield load (Py) to the yield deflection (Δy).The equation 4.1 used is shown below:

$$\text{Initial stiffness} = \frac{Py}{\Delta y} \qquad\qquad 4.1$$

Stiffness calculation is carried out according to Sullivan et al. study (Sullivan et al., 2004). The stiffness results for all stepped beams specimens which are presented in Table 4.2. The results displayed an initial stiffness increment by (1.24–129.96) %. The specimens N and H achieved an increasing in initial stiffness. The ratios of increasing are 129.96% and 53.04% compared to the reference beam, respectively.

The beams with internal steel strengthening, (i.e H-int and H-inc) recorded an initial stiffness of (18 and 17.75) kN/mm and they exhibited a slight increase of stiffness as 3.32% and 1.89 % compared to reference beam Hi, respectively**.**

The stepped beams Nw1 and Hw1, which are strengthened with one layer of cotton belt, achieved initial stiffness of (17.7 and 18.27) kN/mm. i.e. with an increasing ratio 84.18% and 4.87%, higher than reference beams. When two layers of the cotton belt are used as in the Nws2 beam, an initial stiffness increased of 28.43% compared to reference beam. As the compressive strength of the beams changed from normal to high strength, as in the Hws2 beam. The initial stiffness of Nws2 increased by 62.34 % compared to the reference beam. Compared to the reference beam, the beams (Nw2 and Nw2s1) recorded an increase in initial stiffness of (49.84 and 17.48) %. It is noted that the initial stiffness of the stepped beams of high-strength concrete was greater than that of normal strength concrete. The improvement in the stiffness of

reinforced beams is due to the contribution of the cotton belt that restrains crack growth. The initial stiffness increased by (1.24 and 9.98) % compared to reference beams when using carbon fiber sheets as external strengthening of beams (Nc and Ncs). In the strengthening, the use of CFRP sheet is observed to give less initial stiffness than the beams strengthened by the cotton belt. The initial stiffness for all beams is shown in Figure 4.3.

Table 4.2 Initial stiffness for all beams.

Beam remark	Initial stiffness kN/mm	Increasing ratio of stiffness %
Normal strength concrete		
Ni	9.61	-
N	22.10	129.96
Nws2	12.33	28.43
Nw1	17.72	84.18
Nw2	14.44	49.84
Nw2s1	11.29	17.48
Ncs	10.57	9.98
Nc	9.73	1.24
High strength concrete		
Hi	17.42	-
H	26.66	53.04
H-int	18.00	3.32
H-inc	17.75	1.89
Hws2	28.28	62.34
Hw1	18.27	4.87
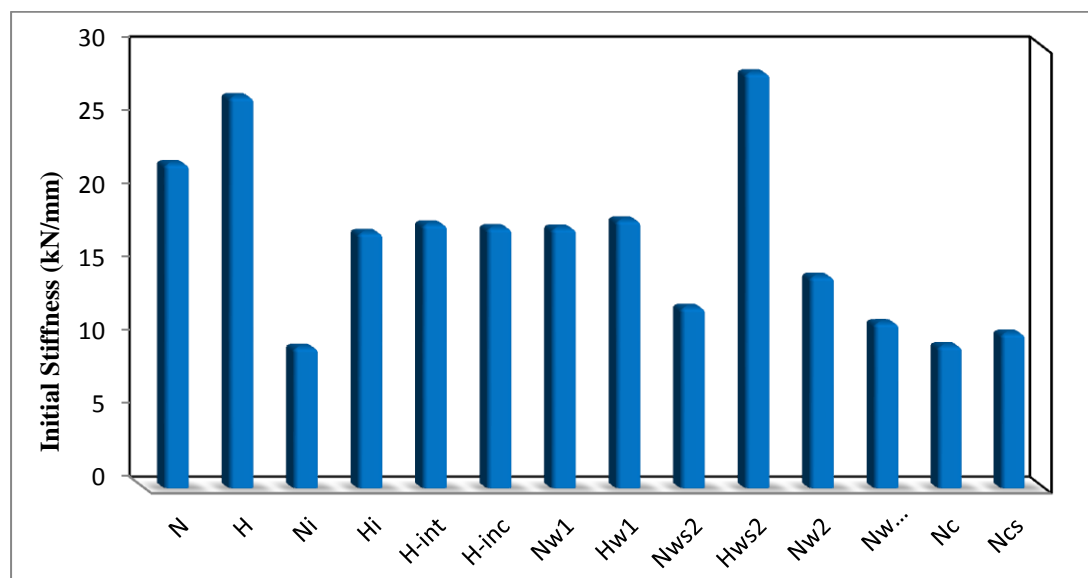
Figure 4.3 Initial stiffness for all beams .

4.4 Ductility index

Ductility is the ability of members to undergo considerable deformations prior to failure. The ductility index (μ) can be obtained from the load-deflection curve, which is equal to the ratio of the maximum deflection (Δu) to the yield deflection(Δy) as can be shown in Figure 4.4.
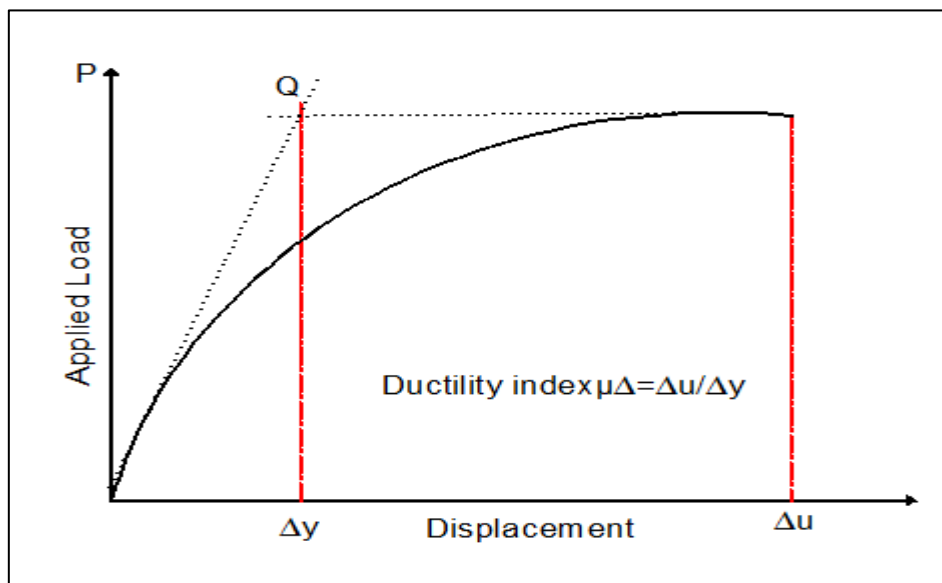
Figure 4.4 Ductility index calculation (Sullivan et al., 2004).

Table 4.3 shows the ductility index for all concrete stepped beams. It is important to note that the used technique for strengthening the stepped beam by cotton belt leads to increases the beam ductility. The beam N has lower ductility index from Ni beam, the lowering ratio 6.82% compared with that of Ni. For beam H, the increasing ratio with respect to the control beam for ductility index is 2.4%.

For the internal strengthening stepped beams, the results showed that the ductility of beams (H-int and H-inc) are (5.658 and 5.827) respectively, with an increase of 32% and 36%, respectively, compared to the reference beam Hi.

For the external strengthening the beams (Nw1 and Hw1) which are strengthened by one layer of the cotton belt recorded ductility of

8.736 and 3.48, respectively. The specimen Nw1 has ductility greater than reference beam by 311.4 %, while the beam Hw1 recorded reduction in ductility by 18.73 % compared to the reference beam. The two-layer cotton belt strengthened stepped beam Nws2 recorded an increase in ductility by 119.78% compared to reference beam. For the same strengthening scheme, and when the concrete compressive strength changed from normal to high as in beam Hws2, it is observed an increase in ductility by 15.84% compared to the reference beam, for beams (Nw2 and Nw2s1) increased in ductility by 94.15 % and 51.91 % respectively relative to the reference beam.

The specimens strengthened by carbon fiber Nc and Ncs achieved ductility of 2.461 and 2.905 with an increment of 15.92% and 36.83% compared to reference beam, respectively. It has been observed that the carbon fiber strengthened beams are less ductile than the beam strengthened by cotton belt. Figure 4.5 showed the ductility index for all beams.
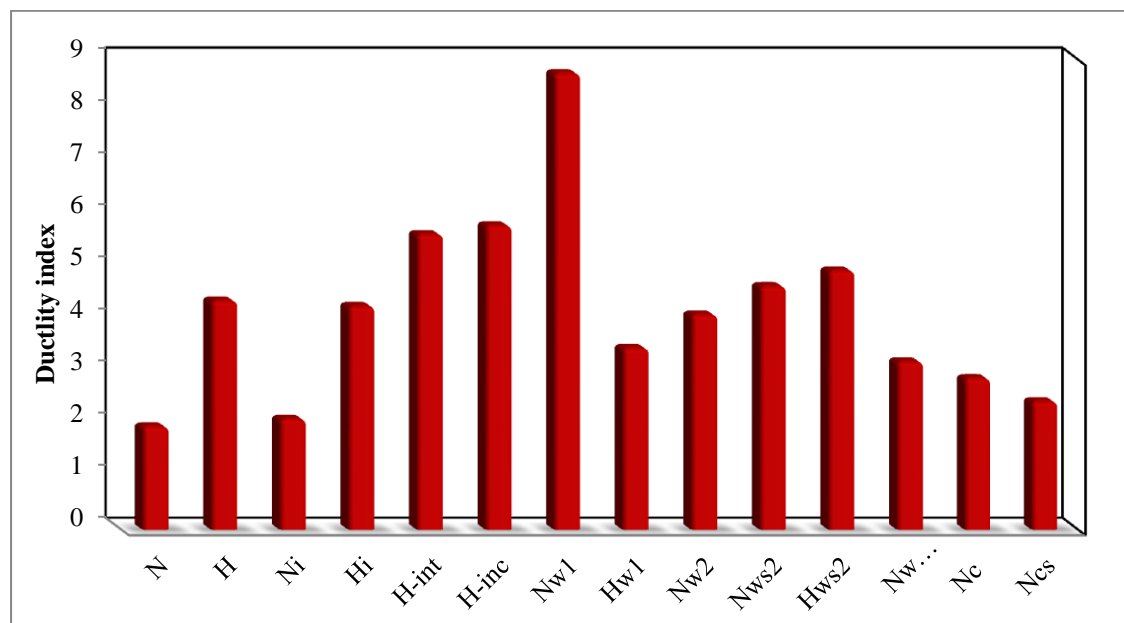
Figure 4.5 Ductility index for all beams.

Table 4.3 Ductility index for all beams

Beam remark	Ultimate Load Pu (kN)	Ductility index	Increasing ratio in ductility %
Normal strength concrete			
Ni	36.2	2.1	-
N	26.3	1.9	-6.8
Nws2	42.5	4.7	119.8
Nw1	51.4	8.7	311.3
Nw2	62.2	4.1	94.2
Nw2s1	54.5	3.3	51.9
Ncs	44.5	2.5	15.9
Nc	58.7	2.9	36.8
High strength concrete			
Hi	39.0	4.3	-
H	37.4	4.4	2.4
H-int	138	5.7	32.1
H-inc	125.4	5.8	35.9
Hws2	70.3	4.9	15.8
Hw1	86	3.5	-18.7

4.5 Energy Absorption

Energy absorption or toughness is the ability of a material to absorb energy and plastically deform action without fracture. One definition of material toughness is the amount of energy per unit volume that a material can absorb before rupturing. The toughness can be defined as the area under the load-deflection curve (Mohy et al., 2013). Table 4.4 presents the energy absorption results (toughness) for all tested beams. The beams N and H are recorded an energy absorption less than reference Ni and Hi beam by (76.18 and 52.19)%, respectively. This reduction is due to change in reinforcement direction from inclination to vertical.

The internal strengthening stepped beams H-int and H-inc are recorded an energy absorption of 3099.62kN.mm and 2326.82kN.mm, i.e. more than reference beams by 1167.73% and 851.66%, respectively, this very large increase in energy absorption is attributed to differences in the internal steel reinforcement details of the stepped joint.

The external strengthening beams Nw1 and Hw1 which are strengthened with one layer of cotton belt recorded greater energy absorption with increments by (574.5 and 138.94)% compared to reference beams, respectively. The beam Nws2 which is strengthened by two-layer of cotton belt recorded energy absorption higher than reference beam by 45%, while the beam Hws2 increase by 41.31% than reference beam. This improvement in absorbed energy is due to change of concrete compressive strength from 45MPa to 85MPa. The stepped beams Nw2s1 and Nw2 achieved energy absorption of 288.487 kN.mm and 346.274 kN.mm with increase ratio (174.88 and 116.38)% compared to reference beam respectively. The results indicated that the one-layer strengthened beams achieved higher energy absorption than the two-layer strengthened beams. This rising in energy absorption of specimens is due to the increase in stiffness after the yield resulted from the cotton belt contribution, which delayed the specimens' failure.

The stepped beams Ncs and Nc which are strengthen with one layer of carbon fiber sheet recorded energy absorption of (180.959 and 428.505) kN.mm with increasing ratios (35.73 and 222.41)% compared to reference beam, respectively. The continuous U-jacket by using belt strips showed a better energy absorption compared to the separated cotton belt and CFRP sheet. Figure 4.6 showed the energy absorption for all beams.
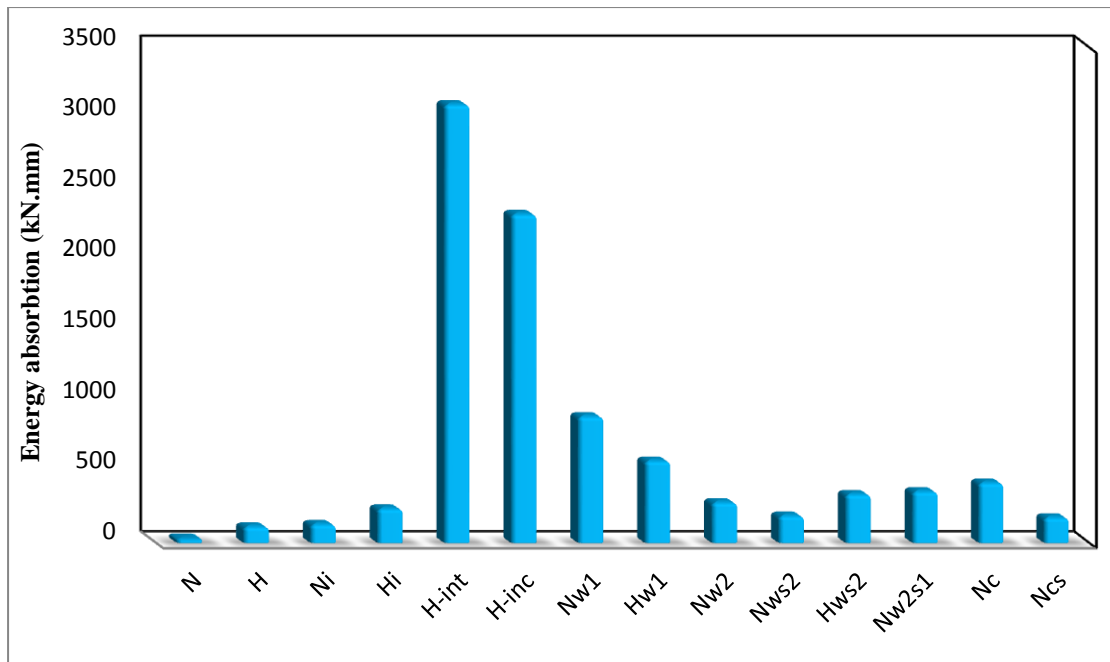
Figure 4.6 Energy absorption for all beams.

Table 4.4 Energy absorption for all beams.

Beam remark	Energy absorption (kN.mm)	Increasing ratio in Energy absorption %
Normal strength concrete		
Ni	133.32	-
N	31.75	-76.18
Nws2	193.4	45.00
Nw1	899.25	574.51
Nw2	288.48	116.38
Nw2s1	366.47	174.88
Ncs	180.95	35.73
Nc	428.50	221.41
High strength concrete		
Hi	244.50	-
H	116.88	-52.19
H-int	3099.61	1167.73
H-inc	2326.82	851.66
Hws2	345.51	41.31
Hw1	584.23	138.94

4.6 Concrete Strain

Data logger device type PFL-30-11 is used to calculate strains of concrete at mid span in compression region. All strain data have been recording by system of data acquisition. The test strains were recorded by direct reading taken by the data acquisition system and 4.2 shows the mathematical method for calculating the strains.

$$\varepsilon = (Ri - R1) \times 10^{-6} \qquad\qquad 4.2$$

where; ε = strain in concrete; Ri = reading at any load; $R1$= initial reading

Table 4.6 shows the strain of concrete at the compression region for all beams. From this table, it is noticed that the compression strain of reference specimens are closed. The results showed that the compression strain at failure load for the internal reinforcement beams H-int and H-inc are the higher strain with value of 0.0026 and 0.002142, than that of reference beams by (277.35 and 210.88)%, respectively.

For stepped beams strengthened with external cotton belt and carbon fiber, the compressive strains are significantly smaller than control specimens at the same load at the service load while at ultimate load the compressive strain is higher than control specimens due to increasing ultimate load for these specimens compared to reference beams. This indicates the positive impact of the strengthening system of the cotton belt and CFRP. The stepped beams Nw1 and Hw1 that were strengthened by one layer of cotton belt recorded an increase of strain by ratios (248.32 and 34.68)% compared to reference beam respectively. The stepped beam Nws2, Nw2, Nw2s1 and Hws2 which were strengthened with two layer of cotton belts recorded an increase in strain by (6.508, 3.35, 18.93 and 1.88)% compared to reference beams, respectively. The

stepped beams strengthened by CFRP sheet Nc and Ncs achieved an increase in strain by (40.03 and 13.21)% compared to reference beam, respectively. It is noted that all the values of the strain at the compression region came within the limits of compressive (crushing) strain, which are less than 0.003.Figure 4.7 clearly depicts strain distribution versus applied stress.

Table 4.5 Strain at failure load for all beams.

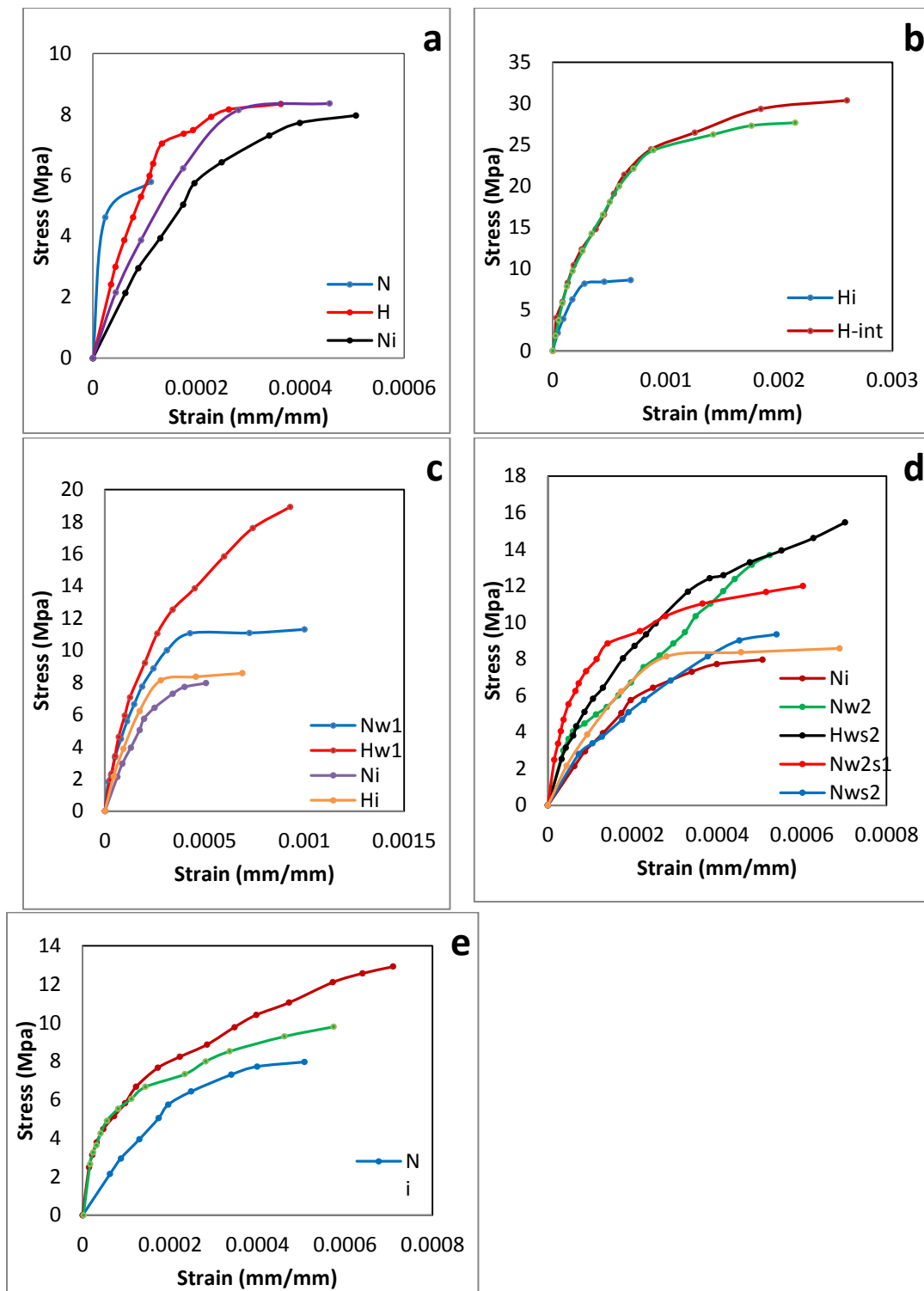| Beam remark	Compressive Strain	Increasing ratio in strain %
Normal concrete strength		
Ni	0.00051	-
N	0.00011	-77.9
Nws2	0.00054	6.5
Nw1	0.00176	248.3
Nw2	0.00052	3.4
Nw2s1	0.00060	18.9
Ncs	0.00057	13.2
Nc	0.00071	40.1
High concrete strength		
Hi	0.000689	-
H	0.00036	-47.5
H-int	0.0026	277.4
H-inc	0.00214	210.9
Hws2	0.00070	1.9
Hw1	0.00093	34.7

Figure 4.7 Strain distribution for all beams

a. Unstrengthened beam, b. Internal strengthening beams.

c. External strengthening beams by one layer of cotton belt.

d. External strengthening beams by two layers of cotton belt.

e. External strengthening beams by CFRP.

Table 4.6 Strain at failure load for all beams.

Beam remark	Compressive Strain	Increasing ratio in strain %
Normal concrete strength		
Ni	0.00051	-
N	0.00011	-77.9
Nws2	0.00054	6.5
Nw1	0.00176	248.3
Nw2	0.00052	3.4
Nw2s1	0.00060	18.9
Ncs	0.00057	13.2
Nc	0.00071	40.1
High concrete strength		
Hi	0.000689	-
H	0.00036	-47.5
H-int	0.0026	277.4
H-inc	0.00214	210.9
Hws2	0.00070	1.9
Hw1	0.00093	34.7

4.7 Crack Propagation and Modes of Failure

Table 4.7 shows cracking load for all beams. The N-beam failure mode is flexural failure where the cracks began to appear in a vertical load of 19 kN on the tension side of the kink of the stepped joint. Then, with the increasing in load led to an increase in the spread and length of the inclined cracks in the stepped joint until the beam completely collapsed as flexural failure mode. When the compressive strength of concrete was changed from normal strength (45 MPa) to high strength (85 MPa) as in the beam H, the crack began to appear at a load of 24 kN, i.e. delay in crack appearance. The beam H showed similar behavior as that of beam N till failure except that the propagation of cracks was less than that of beam H. Cracks began to appear at the stepped joint of beams Ni and Hi at a vertical load of about 23 kN and 28 kN.

As for internal reinforcement is used, it was observed that the spreading of the cracks increased when the steel reinforcement is intensely distributed in the stepped joint as in the beam H-int. The beams H-int and H-inc showed a failure behavior similar to the that of the beam Hi, but with more spread of cracks at the stepped joint.

As for the external strengthening, the stepped beams Nw1 and Hw1 strengthened by one layer of cotton belt started to crack at the vertical load of about 30.2 and 42 kN and the failure mode began in form of a rupture in the cotton belt followed by flexural failure. The results showed that the specimen with high compressive strength and strengthened with the cotton belt gave a better result for the first crack by 39.07 % than the normal strength beam such as beam Hw1. The crack began to appear at stepped joint beams (Nw2, Nws2, Hws2 and Nw2s1) that were strengthened by two layers of cotton belt, at a vertical load of about (22.6, 36.5, 17 and 21.3) kN respectively, while the failure mode was in form of rupture in the cotton belt followed by flexural failure.

Cracks began to appear at the stepped joint in beams Nc and Ncs at a vertical loads of about 30 and 25 kN, respectively. They were followed by the initiation of the vertical sheet rupture of CFRP. No separation noted at the interface between the concrete substrate and the cotton belt or CFRP system and/or between the epoxy and the cotton belt or CFRP in all strengthened specimens. The test of strengthened specimens showed the effect of the cotton belt and CFRP on the situation of failure, the formation and development of cracks. The strengthened cotton belt and CFRP pattern have an important effect on both the mode of failure and beam ultimate load capacity. The strengthening configurations changed the characteristics of failure significantly. Delayed appearance of cracks increased the ultimate capacity. For beam (H-int) showed the best results. Few specimens displayed shear failure mode in addition to flexural

failure mode. Figure 4.8shows the first crack for all beams and Figure 4.9 shows failure patterns for all beams.

Table 4.7 : Crack load for all beams

| Beam remark	Failure load(kN) (Pu)	Crack load (kN) (Pcr)	Pcr/Pu	Mode of failure
N	26.3	19	0.722	Flexural failure
H	37.4	24	0.641	Flexural failure
Ni	36.2	22.9	0.632	Flexural failure
Hi	39	28.3	0.725	Flexural failure
H-int	138	62	0.449	Flexural failure
H-inc	125.7	65	0.517	Flexural failure
Nw1	51.4	30.2	0.587	Rupture of belt strip followed by flexural failure
Hw1	86	42	0.488	Rupture of belt strip followed by flexural failure
Nws2	42.5	17	0.4	Rupture of belt strip followed by flexural failure
Hws2	70.3	36.5	0.519	Rupture of belt strip followed by flexural failure
Ncs	44.5	25.1	0.564	Rupture of carbon fiber followed by flexural failure
Nw2	62.2	22.6	0.363	Rupture of belt strip followed by flexural failure
Nw2s1	54.5	21.3	0.391	Rupture of belt strip followed by flexural failure
Nc	58.7	30.3	0.516	Rupture of carbon fiber followed by flexural failure
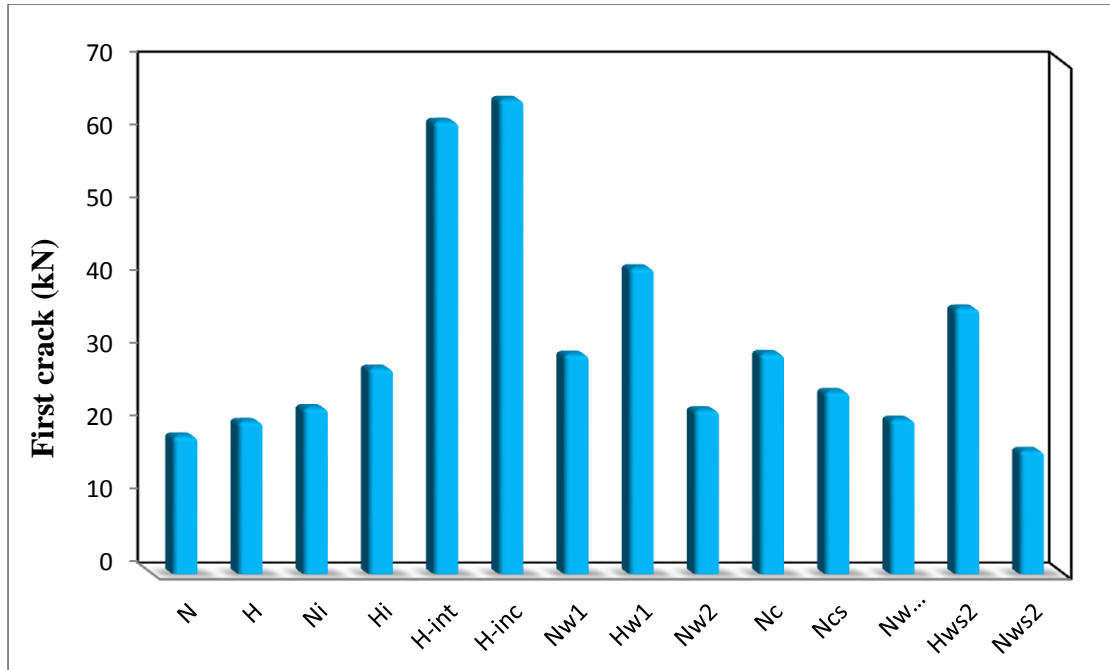
Figure 4.8 First crack for all beams.

Figure 4.9 Cracks pattern for beams.

Fig. 4.9 Continues.

Fig. 4.9 Continues.

CHAPTER FIVE

CONCLUSIONS AND RECOMMENDATIONS

5.1 Conclusions

Based on the experimental investigation of this research, the following remarks can be concluded:

1- The internally strengthened reinforced concrete stepped beams by steel reinforcement generally showed a significant increase in the ultimate loads and deflection. This increase of ultimate load and deflection reached to 253.8 % and 277%, respectively, compared to the reference beam.

2- High strength stepped beam that was strengthened by one layer of cotton belt achieved ultimate load capacity increase of 120%, while beam made of normal concrete strength showed the increase of ultimate load reached to 42% compared to the reference beam.

3- Generally, the externally strengthened reinforced concrete stepped beams made of high concrete strength with two layers of cotton belt showed a significant increase in ultimate load capacity, this increase reached to 80.25 % while the beams made of normal concrete strength showed the increase reached to 72% relative to the reference beam.

4- The increase in the number of cotton belt layers from one layer to two layers led to increase in the cracking and ultimate load capacity.

5- The high strength concrete beams that were strengthened by cotton belts achieved load capacity increment by (80.25-120.5)% compared to normal strength beams, this improvement is attributed to the various properties of high strength concrete in terms of

higher compressive strength and higher tensile strength than normal concrete strength.

6- The externally strengthened reinforced concrete stepped beams with CFRP sheets generally showed a significant increase in the ultimate loads. This increase reaches to 62.15 % compared to reference beam.

7- The reinforced stepped beams strengthened with CFRP sheets and cotton belts show lower deflections at corresponding loads compared to the reference beam.

8- The strengthened cotton belt and CFRP pattern have an important effect on both the mode of failure and beam ultimate load capacity. The continuous configuration of the U-jacket was the best pattern to increase the beam performance than the vertical isolated strips.

9- Overall, the cotton belt showed an increase in beam stiffness compared with reference beam , the gain in the stiffness of the strengthened beams (for different strengthening schemes) ranged from 1.24%-129.96%.

10- The most cracks of the tested beams were concerned in the stepped portion.

11- It is not guaranteed that the CFRP strengthening technique always increases the ultimate capacity of stepped beam. The affirmative effect always happens if only the proper configuration is chosen based on rigorous analysis.

5.2 Recommendations for Future Works

After completion of this investigation, the following recommendations for further research are suggested:

1- Investigating the structural behavior of reinforced concrete stepped beams using sifcon at stepped joint.

2- Studying the effect of using high strength concrete at stepped joint and normal concrete on the structural behavior of hybrid reinforced concrete beams.

3- Investigating the structural behavior of repaired reinforced concrete stepped beams with CFRP laminates.

REFERENCES

Guide for the Design and Construction of Externally Bonded FRP Systems for Strengthening Concrete Structures. 440.2R, A. (2017). 440.2R-17: https://doi.org/10.14359/51700867

Abdel-Moniem, A., Madkour, H., Farah, K., & Abdullah, A. (2018). Numerical Investigation for External Strengthening of Dapped-End Beams. *International Journal of Civil and Environmental Engineering*, *12*(10), 1017-1027.

Al Jawahery, M. S., Gulsan, M. E., Albegmprli, H. M., Mansoori, I. A. H., & Cevik, A. (2019). Experimental investigation of rehabilitated RC haunched beams via CFRP with 3D-FE modeling analysis. *Engineering Structures*, *196*, 109301. https://doi.org/10.1016/j.engstruct.2019.109301

ASTM, C. (1999). 494. Standard Specification for Chemical Admixtures for Concrete. American Society for Testing and Materials.

ASTM A615/A615M-20. (2020). Standard Specification for Deformed and Plain Carbon-Steel Bars for Concrete Reinforcement. https://doi.org/10.1520/A0615.

ASTM C1240-04. 2004. Standard Specification for the Use of Silica Fume as a Mineral Admixture in Hydraulic Cement Concrete, Mortar and Grout. American Society for Testing and Materials. Vol. 4.2, 6p https://doi.org/10.1680/macr.14.00067

Atta, A. M., & El-Shafiey, T. F. (2014). Strengthening of RC dapped-end beams under torsional moment. *Magazine of concrete research*, *66*(20), 1065-1072.

Atta, A., & Taman, M. (2016). Innovative method for strengthening dapped-end beams using an external prestressing technique. *Materials and Structures/Materiaux et Constructions*, *49*(8), 3005–3019. https://doi.org/10.1617/s11527-015-0701-8

Afefy, H. M. E. D., Mahmoud, M. H., & Fawzy, T. M. (2013). Rehabilitation of defected RC stepped beams using CFRP. *Engineering structures*, *49*, 295-305.

Balduzzi, G., Aminbaghai, M., Sacco, E., Füssl, J., Eberhardsteiner, J., & Auricchio, F. (2016). Non-prismatic beams: A simple and effective Timoshenko-like model. *International Journal of Solids and Structures, 90, 236–250.* https://doi.org/10.1016/j.ijsolstr.2016.02.017

BS 1881, P. 116. (1989). Method for determination of compressive strength of concrete cubes. In *British Standards Institution* (p. 3).

C496, A. (2006). "Standard Test Method for Splitting Tensile of

References

Cylindrical Concrete Specimens",. American Society for Testing and Materials.

C78, A. (2002). Standard Test Method for Flexural Strength of Concrete. American Society for Testing and Materials.

de Rooij, M. R., & de Mendonça Filho, F. F. (2015). Dealing with uncertainty in material characterization of concrete by education. *15th Euroseminar on Microscopy Applied to Building Materials, 17-19 June 2015, Delft, The Netherlands, 1-11.*

Fayed, S., Basha, A., & Elsamak, G. (2020). Behavior of RC stepped beams with different configurations: An experimental and numerical study. Structural Concrete, 21(6), 2601–2627. https://doi.org/10.1002/suco.201900503.

Ghosh, S. K. (2004, July). High strength concrete in US codes and standards. In *XIV Congresso Nacional de Ingeniería Estructural* (Vol. 97, No. 4, pp. 1-16).

Gokul, G. A., & Indira, S. (2020). Deformational behavior of high strength concrete (M60) beams using steel fibre under flexural loading

Hussain, M. A., & Safiq, N. (2016, December). Experimental study for stepped reinforcement concrete beams. In *Engineering Challenges for Sustainable Future: Proceedings of the 3rd International Conference on Civil, Offshore and Environmental Engineering (ICCOEE 2016, Malaysia, 15-17 Aug 2016)* (p. 477). CRC Press. https://doi.org/10.1201/b21942-97.

https://www.homeconstructionimprovement.com/stepped footings 6/5/2021

Ibrahim, S. K., & Rad, M. M. (2020). Numerical plastic analysis of non-prismatic reinforced concrete beams strengthened by carbon fiber reinforced polymers. *Proceedings of the 2020 Session of the 13th Fib International PhD Symposium in Civil Engineering, September, 208–215.*

Iraqi Standard No. 5 /1984. Physical and chemical requirements for portland cement.

Iraqi Standard No. 45 /1984. Requirements of the used fine and coarse aggregate in the concrete mixes.

Jaafer, A. A., & Abdulghani, A. W. (2018, December). Nonlinear finite element analysis for reinforced concrete haunched beams with opening. In *IOP Conference Series: Materials Science and Engineering* (Vol. 454, No. 1, p. 012152). IOP Publishing.https://doi.org/10.1088/1757-899X/454/1/012152

Jolly, A., & Vijayan, V. (2016). Structural behaviour of reinforced concrete haunched beam: A study on ANSYS and ETABS. *Int. J. Innovative Sci. Eng. Technol*, 3(8), 495-500.

References

Kovačević, I., & Džidić, S. (2018). High-strength concrete (HSC) material for high-rise buildings. In *12th Scientific Research Symposium with International Participation «Metallic and Nonmetallic Materials: production-properties-application* (No. 12, pp. 214-223).

Mohammed, D H. (2007). Behavior of Reinforced Concrete Beams Strengthened by CFRP in Flexure. Ph. D. Thesis, University of Technology, Iraq.

Meruane, V., & Petrone, G. (2015, April). Mechanical characterisation of a bio-based composite panel. In INTER-NOISE and NOISE-CON Congress and Conference Proceedings (Vol. 251, No. 1, pp. 356-366). Institute of Noise Control Engineering.

Qeshta, I. M. I., Shafigh, P., & Jumaat, M. Z. (2015). Flexural behaviour of RC beams strengthened with wire mesh-epoxy composite. *Construction and Building Materials, 79, 104–114.* https://doi.org/10.1016/j.conbuildmat.2015.01.013

Rentería-soto, J., Cruz-solís, J. J., Betancourt-chávez, J. R., Narayanasamy, R., Fica-ujed, R., Palacio, G., Fi-unach, R., Gutierrez, T., & México, C. (2019). Experimental study of two strut and tie models for dapped -end beams. *International Journal For Technological Research In Engineering Volume 6, Issue 7.*

Rishq & Jaafer (2021). Strengthening and rehabilitation of reinforced concrete joints using polyster belts

Sas, G., Dăescu, C., Popescu, C., & Nagy-György, T. (2014). Numerical optimization of strengthening disturbed regions of dapped-end beams using NSM and EBR CFRP. *Composites Part B: Engineering, 67, 381–390.*

Shree, G., & Kumar, S. (2018). Analysis of stepped beam with multiple transverse cracks. *SSRG International Journal of Civil Engineering (SSRG-IJCE)-Special Issue ICETSST.*
https://doi.org/10.1016/j.compositesb.2014.07.013

Shakir, Q. M., Abd, B. B., & Jasim, A. T. (2018). Experimental and Numerical Investigation of Self Compacting Reinforced Concrete Dapped End Beams Strengthened with CFRP Sheets. *Journal of University of Babylon for Engineering Sciences, 26(7), 16–35.* https://doi.org/10.29196/jubes.v26i7.1482

Shallan, O., Abd-El-Mottaleb, H. E., Mohamed, H. A., & Al-Ashmawy, A. M. (2017). Behavior of stepped reinforced concrete BeamUnder static loads. *Int J Eng Res Technol, 6(02), 196–199.*

Sika. (2017). Sika: Product informationSikadur®-330 - Technical Sheets. May, 2–5.
https://usa.sika.com/content/dam/dms/us01/0/sikadur_-330.pdf

Sullivan, T. J., Calvi, G. M., & Priestley, M. J. N. (2004, August).

References

Initial stiffness versus secant stiffness in displacement based design. In *13th World Conference of Earthquake Engineering (WCEE)* (No. 2888).

Tan, K. H. (2004). Design of non-prismatic RC beams using strut-and-tie models. *Journal of Advanced Concrete Technology*, *2*(2), 249-256.https://doi.org/10.3151/jact.2.249

https://doi.org/10.1016/j.jobe.2020.101757

Tu'ma, N. H., & Aziz, M. R. (2019). Flexural performance of composite ultra-high performance concrete-encased steel hollow beams. *Civil Engineering J*, *5*, 1289–1304.

Webbing. http://www.yaletech.cc/20-lifting-equipments 14/5/2021

Webbing 101: https://www.ballyribbon.com/wp-content/uploads/ebook-webbing 101.pdf

Yousif, M. Z. (2012). R.C. Beams Strengthening by Carbon Fiber Reinforced Polymer Against Two Points Load Divergence. *Journal of Engineering and Development, 16(2), 266–280.*

الخلاصة

تهدف الدراسة الحالية إلى فحص السلوك الإنشائي للعتبات الخرسانية المتدرجة. يتكون العمل
التجريبي لهذا العمل من أربعة عش عتبة متدرجة بأبعاد (العرض، الارتفاع ،الطول)
١٥٠*٣٠٠*٢٣٠٠ ملم تم اختبارها تحت اربع نقاط تحميل. في هذا العمل ، تمت دراسة ثلاثة
متغيرات ، الأول هو مقاومة الانضغاط ، والتي تتضمن قوتين ، 40 ميجا باسكال كمقاومة
انضغاط عادية و 85 ميجا باسكال كمقاومة انضغاط عالية. المتغير الثاني هو تفاصيل حديد
التسليح عند الوصلة المتدرجة حيث تم استخدام حديد تسليح بقطر 8 ملم. تم استخدام تفصيلين
في النموذج الاول ، حديد التسليح بمسافات افقيه ورأسيه 30 و40 ملم على التوالي، وفي
النموذج الثاني بمسافات افقيه ورأسيه ومائله 80 و 75 و50 ملم على التوالي. بينما المتغير
الثالث هو التقوية الخارجية بواسطة حزام قطني (طبقة واحدة او طبقتين من حزام القطن)
ولوح الياف كاربون (CFRP) تمت تقويه ٦ نماذج بالحزام القطني بأنماط تقوية مختلفة
ونموذجين من لوح الياف الكاربون(CFRP).

يتم فحص سلوك العتبات المتدرجة من خلال أنماط الشقوق ، وحمل الشق الأول ، والأحمال
النهائية ، واستجابة انحراف الحمولة ، وتوزيع الانفعالات.

أظهرت النتائج التجريبية زيادة الأحمال النهائية تصل الى 253.84٪ للتقوية الداخلية ذات
مقاومة الانضغاط العالية. اما بالنسبة العتبات التي تم تقويتها بحزام قطني للخرسانة عالية القوة
للخرسانة ذات القوة العادية، والعتبات التي تمت تقويتها بلوح الياف الكاربون(CFRP)
للخرسانة ذات القوة العادية فإنها حققت زياده بالأحمال النهائية بنسبة 120.5٪ و 62.15٪
مقارنه بالعتبة الخرسانية المسلحة غير المقواة (العتبة المرجعية) على التوالي. علاوة على ذلك
، أظهرت هذه العتبات المقواة انحرافًا أقل عند الأحمال المقابلة مقارنة بالعتبة الخرسانية
المسلحة غير المقواة. وقد حققت العينات امتصاصًا للطاقة وليونة وصلابة ابتدائية تتراوح بين
(3100-31.75) كيلو نيوتن ملم ، (8.736 -1.978) و (28.28 -9.61) كيلو نيوتن / ملم
على التوالي. كما أظهرت نتيجة الاختبار زيادات في حمل الشق الأول تصل إلى (129.68)٪
في العتبات المقواة داخليا مقارنة بالعتبة المرجعية.

دراسة عملية للعتبات الخرسانية المسلحة المتدرجة

رسالة
مقدمة الى كلية الهندسة في جامعه ميسان
كجزء من متطلبات الحصول على درجة الماجستير في علوم الهندسة المدنية / الإنشاءات

من قبل
زهراء عبد الحسين موسى
(بكالوريوس هندسة مدنية ٢٠١٧)

بأشراف
الاستاذ الدكتور : عبد الخالق عبد اليمة جعفر

جماد الاخر ١٤٤٣   شباط ٢٠٢١